# OPTICAL CONTROL OF COHERENT QUANTUM SYSTEMS

Colin Dean Roy

Dissertation Prepared for the Degree of

DOCTOR OF PHILOSOPHY

UNIVERSITY OF NORTH TEXAS

December 2022

APPROVED:

Yuri Rostovtsev, Major Professor
Usha Phillipose, Committee Member
Arkadii Krokhin, Committee Member
Paolo Grigolini, Committee Member
Jingbiao Cui, Chair of the Department of Physics
John Quintanilla, Interim Dean of the College of Science
Victor Prybutok, Dean of the Toulouse Graduate School

Roy, Colin Dean. *Optical Control of Coherent Quantum Systems.* Doctor of Philosophy (Physics), December 2022, 59 pp., 16 figures, 76 numbered references.

Optical control of coherent quantum systems has many methods and applications. In this defense we will discuss the effects of an electric field interacting with molecules with dipole moments. The theoretical study of such molecules will consist of two-level atom and a three-level atom in the λ configuration. The methods that will be discussed are population trapping using both bright and dark starts obtained by both STIRAP and CHIRAP pulses. The application to be discussed is how to create a room temperature maser.

ACKNOWLEDGEMENTS

I would like to thank my research advisor Dr. Yuri Rostovtsev for his endless support and patience he has given me the past 5 years. I also want to express gratitude to my defense committee, Dr. Arkadii Krokhin, Dr. Paolo Grigolini, and Dr. Usha Philipose for their taking the time to help me through this dissertation and defense. I want to thank the Physics Department at UNT for allowing me to be part of their program and pursue my goals. I also want to thank my friends and family for the support through this endeavor. Most importantly I would like to express my gratitude to my wife Meranda Roy, without her I would have never attempted this accomplishment.

TABLE OF CONTENTS

# CHAPTER 1

# INTRODUCTION

## 1.1 Introduction

Optics is a broad field of research that is focused on what light is and why it behaves the way it does. Traditional optics takes a geometric approach to the study of light, where light behaves as a ray moving in straight lines. The next progression in the field of optics came when Maxwell formulated the famous Maxwell equations. These equations tell us light is a series of electromagnetic waves that can refract and interfere with itself. Then Einstein turned the world on its head with his theoretical discovery that light is made up of particles called photons. This discovery along with Planck's discovery of quantization lead to quantum mechanics. Quantum mechanics told us that light is indeed made up of photons but that photons like all particles behave as both waves and particles. With the explosion of theoretical and experimental advancement brought on by quantum mechanics lead to quantum optics which is the latest field of optics. Quantum optics is a field of research that focuses on how light interacts with atoms and molecules. One can study how an individual photon interacts with atom or the effect an electromagnetic wave has on atoms and molecules.

To understand the field of quantum optics one needs to understand how an atom is structured, more importantly how the electron behaves within the atom. Atoms are comprised of electrons, protons, and neutrons. The protons and neutrons make up the nucleus, the electron orbits around this nuclear center in what is called an orbital cloud. The electron orbits in a series of orbitals whose shape and distance from the nucleus depend on the amount of energy that the electron is carrying. Therefore, an electron in

a higher orbital will have more energy than an electron in a lower orbital. The key for quantum optics is that the electron can go up or down in orbitals by way of absorbing or emitting photons. This mechanism can be spontaneous, or it can be controlled. One can use this quantum property of absorption and emission to control atomic states. The control of atomic systems has numerous applications in atomic and molecular physics, quantum information, solid-state physics, and classical physics.

1.2 Theory of Atomic Interaction

To study atomic interaction, one needs to know some governing equations. The first is the Schrödinger equation and its hermitian conjugate.

$$|\dot{\psi}\rangle = \frac{-i}{\hbar}\hat{H}|\psi\rangle \tag{1.0}$$

$$\langle\dot{\psi}| = \frac{i}{\hbar}\langle\psi|\hat{H}^{\dagger} \tag{1.1}$$

In the Schrödinger equation we have the first order derivative with respect to time of the wave function itself. From the Schrödinger equation we can derive the density matrix equation of motion for the system. The density operator can be obtained by using the following formula

$$\rho = \sum P_{\psi}|\psi\rangle\langle\psi| \tag{2.0}$$

Taking the first order time dependent derivative of the density operator will give

$$\dot{\rho} = \sum P_{\psi}(|\dot{\psi}\rangle\langle\psi| + |\psi\rangle\langle\dot{\psi}|) \tag{3.0}$$

From here making the substitution for $|\dot{\psi}\rangle$ and $\langle\dot{\psi}|$ from equation 1.0 and 1.1 into the derivative yields

$$\dot{\rho} = \sum P_{\psi}(\frac{-i}{\hbar}\hat{H}|\psi\rangle\langle\psi| + \frac{i}{\hbar}|\psi\rangle\langle\psi|\hat{H}^{\dagger}) \tag{3.1}$$

Using the relation from equation 3 the relation $\hat{H} = \hat{H}^{\dagger}$ we obtain

$$\dot{\rho} = \frac{-i}{\hbar}[H, \rho] \tag{3.2}$$

This is the Louisville-Vonn Neumann equation of motion for the density operator. However, the Louisville-Von Neumann equation itself does not consider spontaneous emission in the atom. To take that into account we can add the decay rates in the form of a matrix $\Gamma$ which will then give the full equation as

$$\dot{\rho} = \frac{-i}{\hbar}[H, \rho] - \frac{1}{2}\{\Gamma, \rho\} \tag{3.3}$$

$$\dot{\rho}_{ij} = -\frac{i}{\hbar}\sum\{H_{ik}\rho_{kj} - \rho_{ik}H_{kj}\} - \frac{1}{2}\sum\{\Gamma_{ik}\rho_{kj} + \rho_{ik}\Gamma_{kj}\} \tag{3.4}$$

The Louisville-Von Neumann equation is used instead of the Schrödinger equation because of the amount of information carried within the equation. It contains both statistical as well as quantum mechanical information [10]. In using either equation (1.1) or (2.0) we need to know the Hamiltonian of the system. The Hamiltonian gives us the energy of the system more importantly how the interaction occurs. When studying atomic interaction, we obtain two different parts for the Hamiltonian. The total Hamiltonian is given as

$$H = H_0 + H_I \tag{4.0}$$

where $H_0$ is the initial energy function of the atom known as the unperturbed Hamiltonian and is of the form

$$H_0 = \frac{p^2}{2m} + V(r) \tag{5.0}$$

In the above equation the first term gives the kinetic energy of the system and the term $V(r)$ accounts for the electrostatic potential that holds the electron in orbit [10]. The dipole approximation has been used due to its simplification of the system. This is valid

when the atom is much smaller than the incident field, that is $\vec{k} \cdot \vec{r} \ll 1$ . With the dipole approximation the interaction Hamiltonian is

$$H_I = -e\vec{r} \cdot \vec{E}(\vec{r}, t) \tag{6.0}$$

where the field is given as.

$$\vec{E}(\vec{r}, t) = \mathcal{E} \cos(vt) \tag{7.0}$$

The general equation of state for a quantum system is

$$|\psi_n\rangle = C_n|n\rangle \tag{8.0}$$

the term $C_n$ is the probability associated with being in the nth state of the system. For this dissertation I employ a three-level system that can be represented as follows.

$$|\psi\rangle = C_a|a\rangle + C_b|b\rangle + C_c|c\rangle \tag{8.1}$$

This state represents a three-level atomic system known as the Lambda model shown below in figure 1.

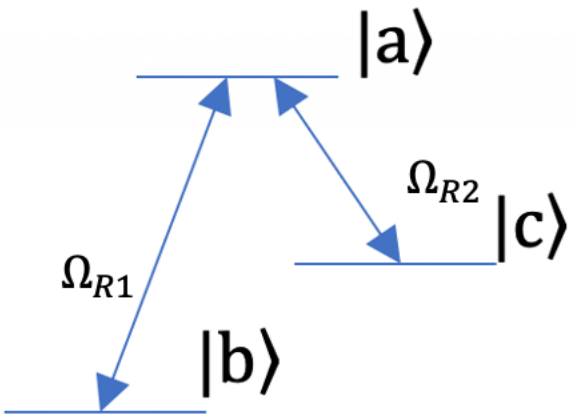


**Figure 1.** The three level Lambda Model with dipole forbidden states $|b\rangle$ $and$ $|c\rangle$ which are both themselves coupled to state $|a\rangle$ by the Rabi frequencies as shown in the figure.

The above three level Lambda model is used to study the effects of coherent quantum systems. In the scheme both states $|b\rangle$ and $|c\rangle$ are coupled to state $|a\rangle$ via an incident

probe pulse $\Omega_{R1}$ and probe pulse $\Omega_{R2}$. Both states $|b\rangle \text{ and } |c\rangle$ are dipole forbidden meaning that there is no direct population transfer to or from either.

There are a few things that need to be shown before we can start to solve this system using either the Schrödinger equation or the Von Neumann equation. The first is the completeness relation given as

$$\sum_n^N |n\rangle \langle n| = 1 \tag{9.0}$$

and for our three level Lambda system the completeness relation is given as.

$$|a\rangle\langle a| + |b\rangle\langle b| + |c\rangle\langle c| = 1 \tag{10.0}$$

By taking this completeness relation we can multiply both sides of the unperturbed Hamiltonian in equation (5.0) and obtain.

$$H_0 = |a\rangle\langle a| + |b\rangle\langle b| + |c\rangle\langle c| H_0 |a\rangle\langle a| + |b\rangle\langle b| + |c\rangle\langle c| \rightarrow$$

$$= \hbar\omega_a |a\rangle\langle a| + \hbar\omega_b |b\rangle\langle b| + \hbar\omega_c |c\rangle\langle c| \tag{5.1}$$

This can then be written out in matrix form for use in the Von Neumann equation.

$$H_0 = \begin{pmatrix} \hbar\omega_a & 0 & 0 \\ 0 & \hbar\omega_b & 0 \\ 0 & 0 & \hbar\omega_c \end{pmatrix} \tag{5.2}$$

We may apply a similar method to the interaction Hamiltonian as well which gives us.

$$H_I = -e[(|a\rangle\langle a| + |b\rangle\langle b| + |c\rangle\langle c|)\vec{r}(|a\rangle\langle a| + |b\rangle\langle b| + |c\rangle\langle c|)]\vec{E}(\vec{r}, t) \rightarrow$$

$$= -[\wp_{ab}|a\rangle\langle b| + \wp_{ac}|a\rangle\langle c| + \wp_{ba}|b\rangle\langle a| + \wp_{ca}|c\rangle\langle a|]E(t) \rightarrow$$

$$= -[\wp_{ab}|a\rangle\langle b| + \wp_{ac}|a\rangle\langle c| + \wp_{ba}|b\rangle\langle a| + \wp_{ca}|c\rangle\langle a|]\mathcal{E}\cos(vt) \tag{6.1}$$

In the above interaction Hamiltonian, the variable $\wp_{ab}$ is the dipole matrix element. It can also be expressed as $\wp_{ab} = |\wp_{ab}|e^{i\phi}$ which benefits with the addition of a phase factor. We can also put the interaction into a matrix as well.

$$H_I = \begin{pmatrix} 0 & -\wp_{ab}E & -\wp_{ac}E \\ -\wp_{ba}E & 0 & 0 \\ -\wp_{ca}E & 0 & 0 \end{pmatrix} \tag{6.2}$$

We can now apply equation 1 to obtain a set of three linear equations shown below.

$$\dot{C_a}(t) = -iC_a(t)\,\omega_a + \frac{i}{\hbar}\wp_{ab}C_b(t)\,\mathcal{E}\cos(vt) + \frac{i}{\hbar}\wp_{ac}C_c(t)\,\mathcal{E}\cos(vt) \tag{11.0}$$

$$\dot{C_b}(t) = -iC_b(t)\,\omega_b + \frac{i}{\hbar}\wp_{ba}C_a(t)\,\mathcal{E}\cos(vt) \tag{11.1}$$

$$\dot{C_c}(t) = -iC_c(t)\,\omega_c + \frac{i}{\hbar}\wp_{ca}C_a(t)\,\mathcal{E}\cos(vt) \tag{11.2}$$

Using the identity $\cos(vt) = \frac{e^{ivt}+e^{-ivt}}{2}$ and $\Omega_R = \frac{|\wp_{ba}|}{\hbar}\mathcal{E}$ we can simplify the set of equations and then solve them. For the papers in chapter 2 and chapter 3 this was done using Mathematica. An important note is that for the research the RWA approximation was used. The RWA gets rid of any terms that oscillate rapidly this is achievable because their average of the rapid oscillations is zero.

To use the Von Neumann equation, one needs to construct the various matrices involved. The first of these is the density matrix which can be obtained using equation 3 and for the Lambda model yields.

$$\rho = \begin{pmatrix} |C_a(t)|^2 & C_a(t)C_b^*(t) & C_a(t)C_c^*(t) \\ C_b(t)C_a^*(t) & |C_b(t)|^2 & C_b(t)C_c^*(t) \\ C_c(t)C_a^*(t) & C_c(t)C_b^*(t) & |C_c(t)|^2 \end{pmatrix} \tag{12.0}$$

The Hamiltonian is given by combining equations 5.2 and 6.2 into equation 4.0 to obtain

$$\begin{pmatrix} \hbar\omega_a & -\wp_{ab}E & -\wp_{ac}E \\ -\wp_{ba}E & \hbar\omega_b & 0 \\ -\wp_{ca}E & 0 & \hbar\omega_c \end{pmatrix} \tag{13.0}$$

Once the equations are found then we can start to solve for them and see the results.

1.3 Coherent Population Trapping Theory

Coherent population trapping (CPT) is the result of a coherent superposition of states. This can lead to some interesting physical results such as dark states and bright states. Dark states and bright states are discussed in more detail in chapter 2. For now, we musst cover the theory of how the dark and bright states are formed. Following the procedure for population trapping outline in [10, 76] and starting with equations 11.0-11.2 we can make a few substitutions $C_a(t) = \tilde{C}_a(t)e^{-i\omega_a t}$, $C_b(t) = \tilde{C}_b(t)e^{-i\omega_b t}$, $C_c(t) = \tilde{C}_c(t)e^{-i\omega_c t}$. We may then differentiate each probability as follows.

$$\dot{C}_a(t) = \dot{\tilde{C}}_a(t)e^{-i\omega_a t} - i\omega_a\tilde{C}_a(t)e^{-i\omega_a t} \tag{14.0}$$

$$\dot{C}_b(t) = \dot{\tilde{C}}_b(t)e^{-i\omega_b t} - i\omega_b\tilde{C}_b(t)e^{-i\omega_b t} \tag{14.1}$$

$$\dot{C}_c(t) = \dot{\tilde{C}}_c(t)e^{-i\omega_c t} - i\omega_c\tilde{C}_c(t)e^{-i\omega_c t} \tag{14.2}$$

These differentiated substitutions can now be put back into equations 11.0-11.2 to yield.

$$\left[\dot{\tilde{C}}_a(t) - i\omega_a\tilde{C}_a(t)\right]e^{-i\omega_a t} = -i\omega_a\tilde{C}_a(t)e^{-i\omega_a t} + i\Omega_{R1}e^{-i\phi}\tilde{C}_b(t)e^{-i\omega_b t}\cos(v_1 t) + i\Omega_{R2}e^{-i\phi}\tilde{C}_c(t)e^{-i\omega_c t}\cos(v_2 t) \tag{15.0}$$

$$\left[\dot{\tilde{C}}_b(t) - i\omega_b\tilde{C}_b(t)\right]e^{-i\omega_b t} = -i\omega_b\tilde{C}_b(t)e^{-i\omega_b t} + i\Omega_{R1}e^{i\phi}\tilde{C}_a(t)e^{-i\omega_a t}\cos(v_1 t) \tag{15.1}$$

$$\left[\dot{\tilde{C}}_c(t) - i\omega_c\tilde{C}_c(t)\right]e^{-i\omega_c t} = -i\omega_c\tilde{C}_c(t)e^{-i\omega_c t} + i\Omega_{R2}e^{i\phi}\tilde{C}_a(t)e^{-i\omega_a t}\cos(v_2 t) \tag{15.2}$$

If we isolate the derivatives and move the rest to the right-hand side. We can then factor out the cosine function and using the RWA ignore any exponential terms containing $(\mathrm{v_n} + \omega_\mathrm{n})$. We also introduce the terms for the energies as $\omega_1 = \omega_\mathrm{a} - \omega_\mathrm{b}, \omega_2 = \omega_\mathrm{a} - \omega_\mathrm{b}$. This will result in the following set of equations

$$\dot{\tilde{C}}_\mathrm{a}(\mathrm{t}) = \frac{\mathrm{i}}{2}\left[\Omega_{\mathrm{R1}}\mathrm{e}^{-\mathrm{i}\phi}\tilde{C}_\mathrm{b}(\mathrm{t})\mathrm{e}^{\mathrm{i}(\mathrm{v}_1-\omega_1)\mathrm{t}} + \Omega_{\mathrm{R2}}\mathrm{e}^{-\mathrm{i}\phi}\tilde{C}_\mathrm{c}(\mathrm{t})\mathrm{e}^{\mathrm{i}(\mathrm{v}_2-\omega_2)\mathrm{t}}\right] \tag{16.0}$$

$$\dot{\tilde{C}}_\mathrm{b}(\mathrm{t}) = \frac{\mathrm{i}}{2}\left[\Omega_{\mathrm{R1}}\mathrm{e}^{\mathrm{i}\phi}\tilde{C}_\mathrm{a}(\mathrm{t})\mathrm{e}^{-\mathrm{i}(\mathrm{v}_1-\omega_1)\mathrm{t}}\right] \tag{16.1}$$

$$\dot{\tilde{C}}_\mathrm{c}(\mathrm{t}) = \frac{\mathrm{i}}{2}\left[\Omega_{\mathrm{R2}}\mathrm{e}^{\mathrm{i}\phi}\tilde{C}_\mathrm{a}(\mathrm{t})\mathrm{e}^{-\mathrm{i}(\mathrm{v}_2-\omega_2)\mathrm{t}}\right] \tag{16.2}$$

Assuming that the fields are resonant with the transition frequency we result in

$$\dot{\tilde{C}}_\mathrm{a}(\mathrm{t}) = \frac{\mathrm{i}}{2}\left[\Omega_{\mathrm{R1}}\mathrm{e}^{-\mathrm{i}\phi}\tilde{C}_\mathrm{b}(\mathrm{t}) + \Omega_{\mathrm{R2}}\mathrm{e}^{-\mathrm{i}\phi}\tilde{C}_\mathrm{c}(\mathrm{t})\right] \tag{17.0}$$

$$\dot{\tilde{C}}_\mathrm{b}(\mathrm{t}) = \frac{\mathrm{i}}{2}\left[\Omega_{\mathrm{R1}}\mathrm{e}^{\mathrm{i}\phi}\tilde{C}_\mathrm{a}(\mathrm{t})\right] \tag{17.1}$$

$$\dot{\tilde{C}}_\mathrm{c}(\mathrm{t}) = \frac{\mathrm{i}}{2}\left[\Omega_{\mathrm{R2}}\mathrm{e}^{\mathrm{i}\phi}\tilde{C}_\mathrm{a}(\mathrm{t})\right] \tag{17.2}$$

which we use to derive our dark and bright states. The first step requires us to take the derivative of $\dot{\tilde{C}}_\mathrm{a}(\mathrm{t})$ to obtain.

$$\ddot{\tilde{C}}_\mathrm{a}(\mathrm{t}) = \frac{\mathrm{i}}{2}\left[\Omega_{\mathrm{R1}}\mathrm{e}^{-\mathrm{i}\phi}\dot{\tilde{C}}_\mathrm{b}(\mathrm{t}) + \Omega_{\mathrm{R2}}\mathrm{e}^{-\mathrm{i}\phi}\dot{\tilde{C}}_\mathrm{c}(\mathrm{t})\right] \tag{18.0}$$

Now we may substitute in equations (17.0-17.2) to obtain

$$\ddot{\tilde{C}}_\mathrm{a}(\mathrm{t}) = \frac{\mathrm{i}}{2}\left[\Omega_{\mathrm{R1}}\mathrm{e}^{-\mathrm{i}\phi}\,\frac{\mathrm{i}}{2}\left[\Omega_{\mathrm{R1}}\mathrm{e}^{\mathrm{i}\phi}\tilde{C}_\mathrm{a}(\mathrm{t})\right] + \Omega_{\mathrm{R2}}\mathrm{e}^{-\mathrm{i}\phi}\,\frac{\mathrm{i}}{2}\left[\Omega_{\mathrm{R2}}\mathrm{e}^{\mathrm{i}\phi}\tilde{C}_\mathrm{a}(\mathrm{t})\right]\right]$$

$$= -\frac{1}{4}\left[\Omega_{\mathrm{R1}}^2\tilde{C}_\mathrm{a}(\mathrm{t}) + \Omega_{\mathrm{R2}}^2\tilde{C}_\mathrm{a}(\mathrm{t})\right] \tag{19.0}$$

using the relationship that $\Omega_\mathrm{R} = \sqrt{\Omega_{\mathrm{R1}}^2 + \Omega_{\mathrm{R2}}^2}$ we obtain.

$$\ddot{\tilde{C}}_\mathrm{a}(\mathrm{t}) = -\frac{1}{4}\Omega_\mathrm{R}^2\tilde{C}_\mathrm{a}(\mathrm{t}) \tag{20.0}$$

$$\ddot{\tilde{C}}_\mathrm{a}(\mathrm{t}) + \frac{1}{4}\Omega_\mathrm{R}^2\tilde{C}_\mathrm{a}(\mathrm{t}) = 0 \tag{20.1}$$

This result looks identical to the equation for a simple harmonic oscillator and can be solved as such. Using the known solution of a simple harmonic oscillator the probability $\tilde{C}_a$ can be written as

$$\tilde{C}_a(t) = A\cos\left(\frac{\Omega_R t}{2}\right) + B\sin\left(\frac{\Omega_R t}{2}\right) \tag{21.0}$$

Common practice in texts and literature set the initial conditions of the atom at $t = 0$ to be a combination of sines and cosines in states $|b\rangle \text{ and } |c\rangle$. The approach used here is from [10] and sets the initial condition as

$$|\psi(0)\rangle = \cos\left(\frac{\theta}{2}\right)|b\rangle + \sin\left(\frac{\theta}{2}\right)e^{-i\psi}|c\rangle \tag{22.0}$$

which leads to the following set of equations for the probability of each state.

$$\tilde{C}_a(t) = \frac{i\sin\left(\frac{\Omega t}{2}\right)}{\Omega}[\Omega_{R1}e^{-i\phi_1}\cos\left(\frac{\theta}{2}\right) + \Omega_{R2}e^{-i(\phi_2+\psi)}\sin\left(\frac{\theta}{2}\right) \tag{23.0}$$

$$\tilde{C}_b(t) = \frac{1}{\Omega^2}\left\{\left[\Omega_{R2}^2 + \Omega_{R1}^2\cos\left(\frac{\Omega t}{2}\right)\right]\cos\left(\frac{\theta}{2}\right) - 2\Omega_{R1}\Omega_{R2}e^{i(\phi_1-\phi_2-\psi)}\sin^2\left(\frac{\Omega t}{4}\right)\sin\left(\frac{\theta}{2}\right)\right\} \tag{23.1}$$

$$\tilde{C}_c(t) = \frac{1}{\Omega^2}\left\{\left[\Omega_{R1}^2 + \Omega_{R2}^2\cos\left(\frac{\Omega t}{2}\right)\right]e^{-i\psi}\sin\left(\frac{\theta}{2}\right) - 2\Omega_{R1}\Omega_{R2}e^{i(\phi_1-\phi_2)}\sin^2\left(\frac{\Omega t}{4}\right)\cos\left(\frac{\theta}{2}\right)\right\} \tag{23.2}$$

If we then set $\Omega_{R1} = \Omega_{R2}$, $\theta = \frac{\pi}{2}$, and $\phi_1 - \phi_2 - \psi = \pm\pi$ we obtain $\tilde{C}_a(t) = 0, \tilde{C}_b(t) = \frac{1}{\sqrt{2}}$, and $\tilde{C}_c(t) = \frac{1}{\sqrt{2}}e^{-i\psi}$. This is what is known as a dark state created using population trapping. In this state the atom is stuck in the $\tilde{C}_b(t) \text{ and } \tilde{C}_c(t)$ states. The use of coherent population trapping, and the methods of bright and dark states will be discussed in more detail in chapter 2.

## 1.4 STIRAP and CHIRAP

There are very powerful techniques when it comes to optical control. One such technique is known as stimulated raman adiabatic passage (STIRAP). STIRAP allows for selective population transfer between quantum states without suffering loss due to spontaneous emission [53]. We can study STIRAP using the Lambda model shown in figure 4 with the two separate pulses needed to achieve population transfer. STIRAP is used to obtain population inversion between two dipole forbidden states by way of coherent population trapping (CPT). In the figure the two pulses will couple their respective population states and allow state $|\mathrm{a}\rangle$ to be passed over with minimal to no excitation depending on the tuning parameters. Another very powerful tool that is used to accompany and help STIRAP achieve this is known as chirped raman adiabatic passage (CHIRAP). In chapter 2 I talk about STIRAP and CHIRAP together. To achieve STIRAP we first need to have our pulse that couples states $|\mathrm{a}\rangle \text{ and } |\mathrm{c}\rangle$ interact with the atom. This will start the coherence between the two levels. Then we must send in our second pulse which will couple states $|\mathrm{a}\rangle \text{ and } |\mathrm{b}\rangle$. This will induce a linkage between our two dipole forbidden states. We use gaussian pulses each separated from one another by time. The pulses have the form of

$$\Omega_{\mathrm{R_i}} = \frac{|\wp_{\mathrm{ij}}|}{\hbar}\mathcal{E}\omega_0 \mathrm{Exp}[-\left(\frac{\mathrm{t}-\frac{\mathrm{tend}}{2}\pm \mathrm{ddt}}{\mathrm{dt}}\right)^2] \tag{24.0}$$

with some familiar variables from our theoretical model. The variable $\frac{\mathrm{tend}}{2}$ is the duration of the pulse divided by two to ensure the pulse peaks in the middle. The variable ddt is used to shift the pulse to the left or right. Since we have two pulses, we separate them as shown in figure 2. The variable dt is just the gaussian duration of the pulse itself.

Lastly $\wp_{ij}$ is the dipole transition matrix element. In figure 2 we show the temporal separation between the two pulses $\Omega_{R1}$ and $\Omega_{R2}$.

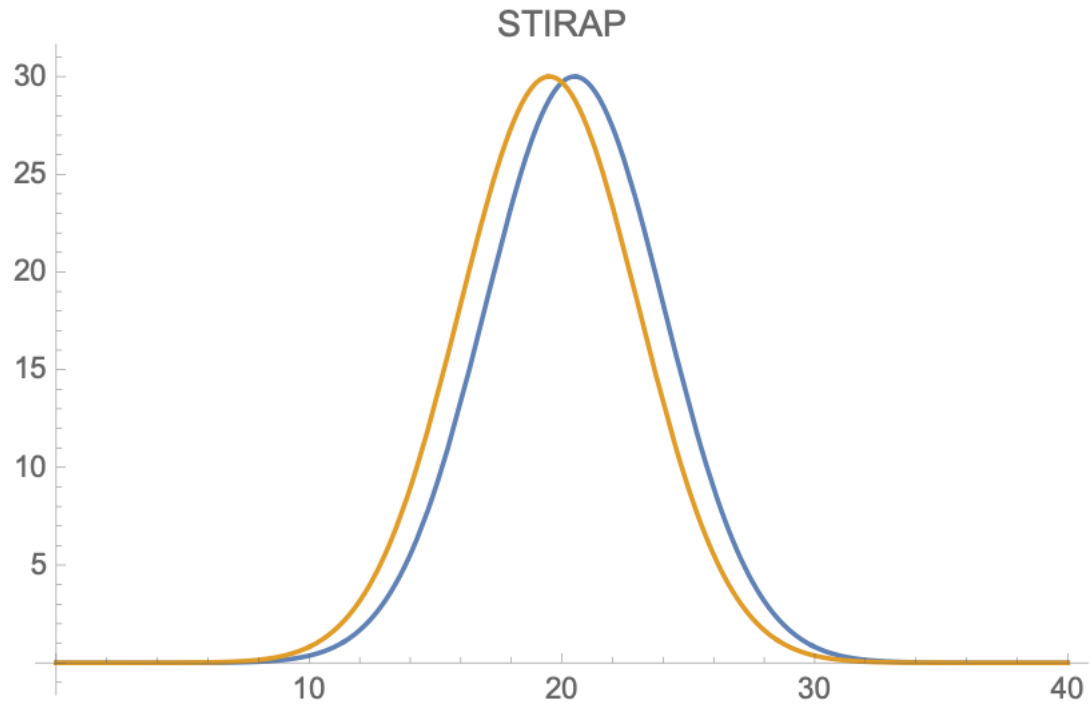


**Figure 2**: Temporally separated adiabatic gaussian pulses $\Omega_{R_i}$ from equation 24.0

The next step is to add the CHIRAP pulse to the model and that pulse is of the form

$$\phi_i = \exp\left[-i\alpha\left(t - \frac{tend}{2}\right)^2\right] \qquad (25.0)$$

In our pulse we have only added an imaginary function and our chirping parameter $\alpha$ the pulse itself is shown in figure 3.

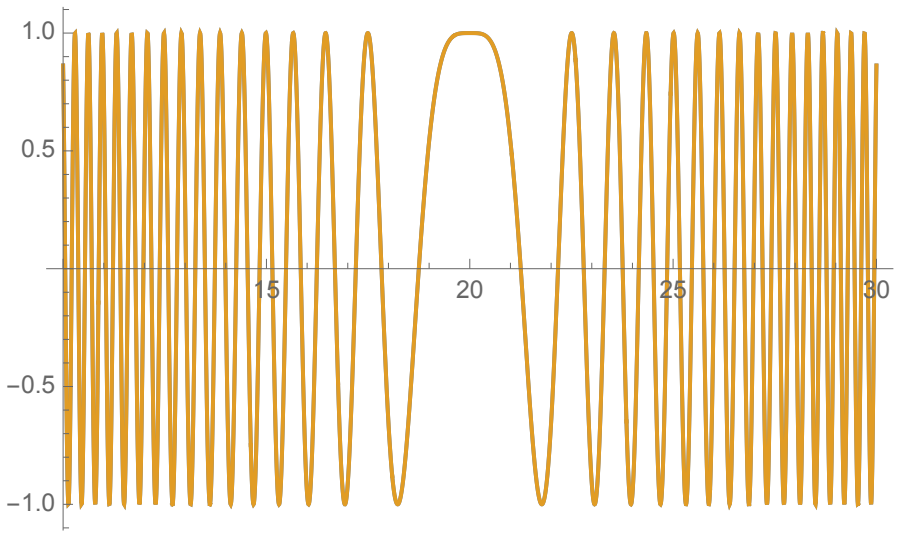


**Figure 3**: Plot of the oscillating CHIRAP pulse $\phi_i$

As briefly discussed, these two techniques have become powerful tools for fields such as quantum information, chemistry, solid state physics, and classical physics. We see that STIRAP on its own is a very powerful technique to induce population inversion between two dipole forbidden states. It is when we introduce the CHIRAP that we see the two together. The chirp pulse acts as a boost for the STIRAP effect.

The rest of this paper is organized as follows. Chapter 2 I focus on STIRAP and the effect of adding a CHIRAP pulse in a three-level lambda model. We see various levels of control that we can obtain with different pulse delay parameters and chirp parameters. We explore both our STIRAP and CHIRAP pulse efficiency in a dense molecular medium. Chapter 3 we focus in two parts, the first deals with how to use our methods of control from chapter 2 for increased molecular detection. The second part of chapter 3 covers our proposed model for a room temperature maser. In chapter 4 we discuss our results and conclusions as well as future avenues of research.

# CHAPTER 2

# COHERENT POPULATION TRAPPING IN MOLECULAR MEDIA

## 2.1 Introduction

Nonlinear optics from the quantum coherence generated by laser excitation via the one-photon and two-photon resonances of atomic or molecular levels is a broad area of research. For example, Raman spectroscopy [27-29] is one among many powerful techniques that has been widely used in engineering, chemical, and biological application specifically employing ultrashort pulses [30]. In an effort to exploit the large bandwidth associated with the short pulses and improve the Raman spectroscopy, newer techniques such as chirped optical pulses are evolved such that the pulse bandwidth can be mapped into the time domain [31]. Using such adaptive techniques for short pulses (e.g., femtosecond duration) allows researchers to excite maximal rotational-vibrational coherence [32] to improve the sensitivity of coherent Raman spectroscopy and to perform real time identification of bacterial spores and biomolecules [19,33-36]. The femtosecond-laser-based coherent anti-stokes Raman spectroscopy (CARS) has been used extensively in time-resolved nonlinear spectroscopy research in recent years [37]. It is used in several fields of study, such as identifying molecules in chemistry, measuring temperature in solid-state physics, and non-invasive monitoring of muscle tissue, among other things [38].

The quantum coherence effects, such as coherent population trapping (CPT) [9] and electromagnetically induced transparency (EIT) [10-12, 39], have the ability to drastically change optical properties of media. For example, for EIT in CW and pulsed regimes [11,12,39-41], absorption practically vanishes. The fluorescence [42] and

photon correlation properties [43] are modified in presence of such quantum coherence. Also, the propagation dynamics of pulses in coherently prepared media has been exploited for nonlinear cross-talks and parametric generations [44].

The medium with excited quantum coherence [10] shows ultra-dispersive properties [13], which causes several orders of magnitude higher spectral dispersion effect than natural material [45]. The corresponding steep dispersion results in the ultra-slow or fast propagation of light pulses, [14-18], which can be used for drastic modification of the phase-matching conditions for Brillouin scattering [47] and four-wave mixing [49]. It has been shown that the optical $0\pi$-pulses [50] under conditions of EIT [51,52] are very sensitive to resonant interaction, and have advantages to be used in quantum sensing, quantum control, optical spectroscopy, and quantum information processing.

The coherent excitation and return to the ground state experienced by two-level atoms exposed to precisely resonant laser pulses with an area of $2\pi$ results in the well-known Self-Induced Transparency (SIT) phenomenon a stable propagation of light pulses without considerable attenuation [32]. Another important example of a possible selective control of population on the molecular levels is referred to as Stimulated Raman Adiabatic Passage (STIRAP) [53-55] that occurs by applying two short laser pulses properly shaped. There is a modification of the technique, the so-called fractional STIRAP, that allows researchers to reach robust control on the molecular coherence excited by laser pulses. It was theoretically shown that the chirped laser pulses, or even a single linearly chirped laser pulse, can be used for an efficient manipulation of atomic population in ultracold Rb atoms [56,57].

In this chapter, we study chirped pulse propagation in presence of the quantum coherence in a $\Lambda$-type molecular media. We have considered the three-level molecules and employ the dressed state approach to obtain physical insight showing interaction of “bright” and “dark states with radiation. The presented model is common for the molecular media, where the split ground states could correspond to the rotational-vibrational levels of a molecule. We demonstrate the role of dark states in propagation of the chirped pulse. The obtained results can be applied to implementation of control of the quantum states and the quantum information in the medium by using the short-pulse laser (see, for example [58]).

Some work has already been done in this area. In the paper [59], the authors investigate the behavior of a three-level atomic system with Lambda structure of levels in the field of a sequence of short frequency-chirped bichromatic laser pulses in the adiabatic passage regime of interaction. The efficiency of the population transfer in this atomic system has been shown to be sensitive to the relative phase of the pulses. This sensitivity can be used for coherent fast and robust writing and reading of optical phase information. This initial preparation of the atom in the “dark” superposition state is suggest through the action of a sequence of a few frequency-chirped pulses with duration longer than the atomic relaxation.

A scheme of population transfer between two metastable (ground) states of the Lambda atom without considerable excitation of the atom using single frequency-chirped laser pulses is presented in [60]. The physics of the process is excitation of the "trapped" superposition of the ground states by the laser pulse at sufficiently high laser peak intensity. During the frequency chirp, the laser pulse must first come into resonance with

the transition from the initially occupied ground state to the excited state and after that with the transition between the excited and second initially empty ground states. In the case when the envelope frequency spectrum width (without chirp) of the pulse exceeds the frequency interval between the two ground states, it was shown a possibility of controllable generation of superposition of the ground states with a controllable excitation of the Lambda atom.

The propagation of frequency-chirped laser pulses in optically thick media was studied in [61]. The authors considered a medium of atoms with a Lambda level scheme (Lambda atoms) and, for comparison, a medium of two-level atoms. Frequency-chirped laser pulses that induce adiabatic population transfer between the atomic levels are considered. They induce transitions between the two lower (metastable) levels of the Lambda atoms and between the ground and excited states of the two-level atoms. It was shown that associated with this adiabatic population transfer in Lambda-atoms, a regime of enhanced transparency of the medium-the pulses occurs when the pulses are distorted much less than in the medium of two-level atoms and retain their ability to transfer the atomic population much longer during propagation.

In the papers [62,63], it was shown that traditional schemes for coherent population transfer or generation of coherent superposition states in multilevel atoms or molecules usually utilize two or more laser beams with radiation bandwidth smaller than the frequency interval between the working levels. The possibility of creation of the coherent superposition of three metastable states of a four-level atom with tripod like level structure using a single short frequency-chirped laser pulse has been shown. No appreciable excitation of the atom takes place during the creation of the coherent

superposition state, thus significantly diminishing the effect of decoherence due to the spontaneous decay of the excited state. The proposed method of creation of superposition states is robust against variations in the laser pulse parameters. Since this method does not require maintaining steady resonance with the atomic transitions (owing to the frequency chirp of the laser pulse), it is effective both in homogeneously and inhomogeneously broadened media.

The simultaneous propagation of a pair of Raman resonant, frequency-modulated (chirped) laser pulses in an optically thick medium, modeled by an ensemble of Lambda atoms have been studied in [64]. A self-organization ("matching") effect is shown for the chirped pulse pair, which leads to a quasilossless propagation. Furthermore, it was demonstrated that a well-defined coherent superposition of the atomic ground states and, correspondingly, a coherence are robustly created in the medium that can be controlled by amplitudes of the laser pulses. The proposed scheme can be applied to substantially increase the efficiency of the optical wave mixing processes, as well as in other nonlinear processes where the initial preparation of a spatially extended medium in a coherent superposition state is required.

In this chapter, we consider the effects of dispersion that occur due to the propagation of the chirped pulses that are detuned from the one-photon resonances. The effects can be strong in a dense medium. We study the propagation of a pair if chirped pulses in the atomic/molecular media that are a gas of three-level quantum system in the $\Lambda$-level configuration. Under the action of the pulses that have same chirping, the physics is similar to the two adiabatic pulses that interacting with quantum system forcing the evolution of the dark state and practically not changing themselves.

Under the action of the pulses that have chirping of the opposite signs, the propagation becomes more interesting with dispersion effects involved. One type of the effect related to the large Rabi frequencies of the pulses that leads to the frequency change of the pulses during propagation.

The second effect is related to this frequency change, it changes the efficiency of the population transfer to totally zero at some distance and then after some propagation distance restores population transfer to the very high level again. These effects have not been discussed yet (to the best of our knowledge). Below we present the change of the phase of the pulses and how it changes the instantaneous frequencies of the pulse while the pulses are propagating

The chapter is organized as follows. In section 2.2, we describe the theoretical model. In section 2.3, we describe the coherent population manipulation and its role for the excitation of the quantum coherence, and we have shown that the presence of the additional levels strongly influence the population transfer as well as the excitation of the population and the coherence. Section 2.4 extends the discussion to propagation of optical fields in both 2 and 3-level systems.

## 2.2 Model

To describe the interaction of the molecules with optical fields we employ molecular model of a three-level quantum system shown in Figure 13 (optical fields are shown in Figure 13(E)). Let us consider a $\Lambda$-type atomic medium. A strong field of frequency $\omega_2$ is the coupling field and a field of frequency $\omega_1$ is the probe field. The probe and coupling fields can be represented as

$$E_{1,2} = E_{1,2}^{0} \exp\left[ik_{1,2}z - i\omega_{1,2}t\right] \tag{26.0}$$

where $E_{1,2}^{0}$ is the amplitudes of fields at z = 0. The interaction Hamiltonian in the rotating wave approximation can be written as

$$H = \hbar\left[\Omega_1^* e^{i\Delta_1 t}|b\rangle\langle a| + \Omega_2^* e^{i\Delta_2 t}|c\rangle\langle a| + \text{ adj.}\right] \tag{27.0}$$

where $|b\rangle\langle a|$, and $|c\rangle\langle a|$ are the atomic projection operators, $\Omega_1 = \wp_{ab}\, E_1/\hbar$ and $\Omega_1 = \wp_{ac}\, E_2/\hbar$ are the probe and coupling Rabi frequencies, $\Delta_1 = \omega_{ab} - \omega_1$ and $\Delta_2 = \omega_{ac} - \omega_2$ are the detunings for probe and coupling laser beams, and $\wp_{ab}$ and $\wp_{ab}$ are the dipole momenta of the corresponding transitions. Here $\omega_{ab}$ and $\omega_{ac}$ are the angular frequency of $|a\rangle \rightarrow |b\rangle$ and $|a\rangle \rightarrow |c\rangle$ transitions. The coupling field is resonant with the $|a\rangle \rightarrow |c\rangle$ transition ($\Delta_2 = 0$). We consider various relations with the duration of the laser pulses and relaxation times. For the case when the laser pulses are shorter than the relaxation times we are going to use the state vector approach. The molecular system in Hamiltonian in Eq. (27.0) is described by the state vector

$$|\psi\rangle = a|a\rangle + b|b\rangle + c|c\rangle \tag{28.0}$$

where a, b, c are the probability amplitudes of the molecular states $|a\rangle$, $|b\rangle$, and $|c\rangle$, respectively. The Schrödinger equation for the state vector is given by

$$i\hbar\frac{\partial}{\partial t}|\psi\rangle = \hat{H}|\psi\rangle \tag{29.0}$$

To take into account the relaxation processes we employ the density matrix approach and the equation are given by

$$\frac{\partial \rho}{\partial t} = \frac{i}{\hbar}[\rho, H] - \Gamma[\rho] \tag{30.0}$$

where $\Gamma[\rho]$ is the relaxation matrix with relaxation rates for all components of the density matrix $\rho$.

The density matrix equations for coherences are given by

$$\dot{\rho}_{ab} = -\Gamma_{ab}\rho_{ab} + i\Omega_1 n_{ab} - i\Omega_2^*\rho_{cb} \tag{31.1}$$

$$\dot{\rho}_{ca} = -\Gamma_{ca}\rho_{ca} + i\Omega_2^* n_{ca} + i\Omega_1^* \rho_{cb} \quad (31.2)$$

$$\dot{\rho}_{cb} = -\Gamma_{cb}\rho_{cb} - i\Omega_2 \rho_{ab} + i\Omega_1 \rho_{ca} \quad (31.3)$$

where $\Gamma_{ca} = \gamma_{ca} - i(\omega_{ac} - \omega_2), \Gamma_{cb} = \gamma_{cb} + i(\omega_{cb} - \omega_1 + \omega_2),$ and $\Gamma_{ab} = \gamma_{ab} + i(\omega_{ab} - \omega_1)$ , $n_{\alpha\beta} = \rho_{\alpha\alpha} - \rho_{\beta\beta}$. The density matrix equations for diagonal elements are given by

$$\dot{\rho}_{aa} = -(\gamma_1 + \gamma_2)\rho_{aa} - 2\Im(\Omega_1 \rho_{ab}) + 2\Im(\Omega_2 \rho_{ac}) \quad (32.1)$$

$$\dot{\rho}_{bb} = \gamma_1 \rho_{aa} + 2\Im(\Omega_1^* \rho_{ab}) \quad (32.2)$$

$$\dot{\rho}_{cc} = \gamma_2 \rho_{aa} - 2\Im(\Omega_2 \rho_{ca}) \quad (32.3)$$

where $\gamma_{1,2}$ are the spontaneous emission relaxation rates for corresponding transitions.

The evolution of optical fields is determined by the propagation equations

$$\frac{\partial \Omega_1}{\partial z} + \frac{1}{c}\frac{\partial \Omega_1}{\partial t} = -i\eta_1 \rho_{ab} \quad (33.0)$$

$$\frac{\partial \Omega_2}{\partial z} + \frac{1}{c}\frac{\partial \Omega_2}{\partial t} = -i\eta_2 \rho_{ac} \quad (34.0)$$

where $\eta_{1,2} = \frac{3\lambda_{1,2}^2 N}{8\pi}\gamma_{1,2}$; To incorporate molecular motions, the doppler broadening is important to take into account by averaging the polarizations $\rho_{ab}$ and $\rho_{ca}$ over the velocity distribution [48]. The optical density is the parameter $D = \frac{3\lambda^2 N}{8\pi} l$ ($l$ is the thickness of the medium) that has a simple physical meaning showing the linear absorption of the weak probe pulse, as it follows from Eq. (31.1) and Eq. (33.0), $\Omega_1(l) = \Omega_1(0)\exp[-D]$, $\Omega_1(0)$ is the field at the entrance of the medium, and $\Omega_1(l)$ is the field at the exit from the medium

2.3 Coherent Population Trapping

First, let us consider the molecular system shown in Fig. 1(A). The state vector is given by Eq. (28.0) and a, b and c coefficients can be found from the set of equations

$$\dot{a} = -i\Omega_1 b - i\Omega_2 c \tag{35.1}$$

$$\dot{b} = -i\Omega_1 a \tag{35.2}$$

$$\dot{c} = -i\Omega_2 a \tag{35.3}$$

Rewriting the equations (35.1-35.3) in terms of the bright and dark states, that can be re-written as

$$\dot{a} = -i\Omega_e B \tag{36.1}$$

$$\dot{B} = -i\Omega_e a + gD \tag{36.2}$$

$$\dot{D} = -gB \tag{36.3}$$

where the coupling g is

$$g = \frac{\dot{\Omega}_1\Omega_2 - \Omega_1\dot{\Omega}_2}{\Omega_1^2 + \Omega_2^2} = \dot{\Theta} \tag{37.0}$$

And $\Theta = \arctan\left(\frac{\Omega_1}{\Omega_2}\right)$. Note that g describes the coupling between the "bright" and "dark" states. Although, we should point out that for the adiabatic pulses, $g \simeq 0$, the excited level $a \simeq 0$ and thus the bright state $B \simeq 0$ is not excited.

Usually, with a weak laser field, the three-level atom is a good approximation. The effect of a stronger laser field coupling additional co-vibrational molecular levels has been discussed in [50][68]. It has been observed that the vibrational Raman transition saturates before the maximal coherence is reached because of the rotational Raman saturation [51][69].

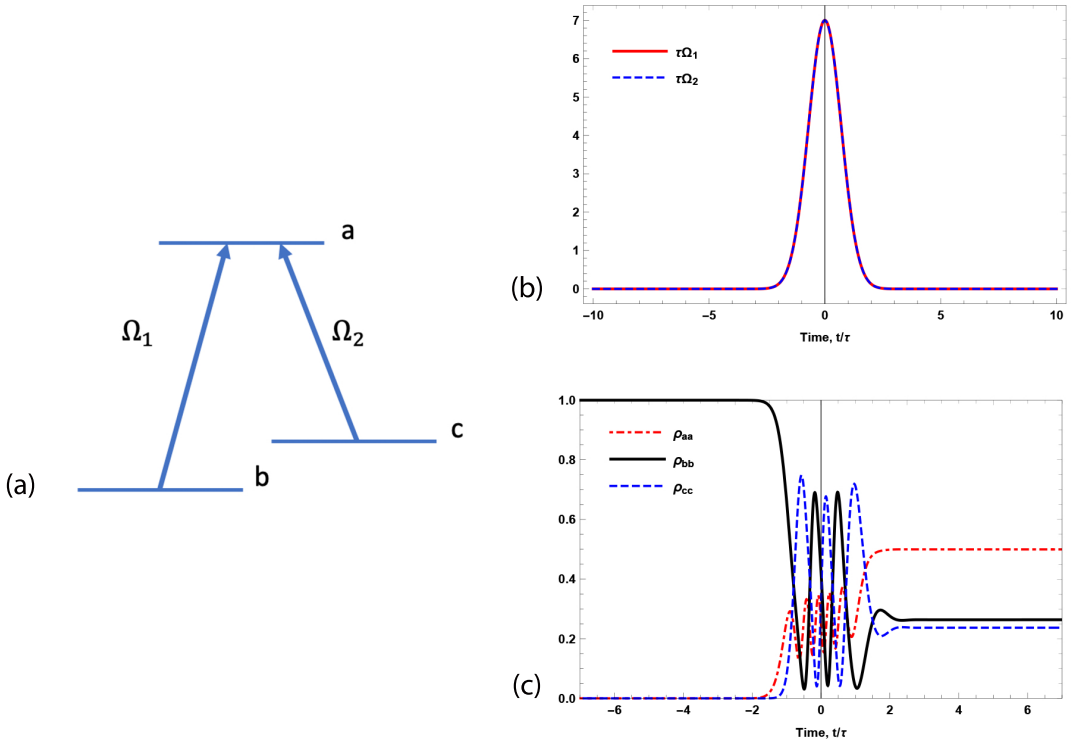


**Figure 4:** (a) The schematic of the bare states of a three-level quantum system is shown that interacts with the same chirped pulse. (b) The pulses $\Omega_1$ and $\Omega_2$ have the same chirping parameters $\alpha_1 = \alpha_2$. (c) The population dynamics of all levels is shown. We can see that the excited state is populated via interacting with chirped pulse, and the coherence between ground states is related to forming a dark state.

It would be interesting to study the modification of control of the quantum system with more general waveform of the adiabatic pulses that include that phase modulation as well. The temporal spread of the laser pulses are shown in Figure 13(E). The gaussian pulses $\Omega_1$ and $\Omega_2$ are given by

$$\Omega_1(t) = \Omega_{10} \exp\left[-\frac{t^2}{2\tau^2} + i\Phi_1\right] \tag{38.1}$$

$$\Omega_2(t) = \Omega_{20} \exp\left[-\frac{(t-\tau_d)^2}{2\tau^2} + i\Phi_2\right] \tag{38.2}$$

where $\tau_d$ is the relative delay time between the laser pulses that have time duration $\tau$, and $\Omega_{10}$ and $\Omega_{20}$ are the complex amplitude of the Gaussian pulses and $\Phi_{1,2} = \alpha_{1,2}t^2$ describe the phase modulation. We can see that for these pulses the population is transferred to close to 100% efficiency as shown below.

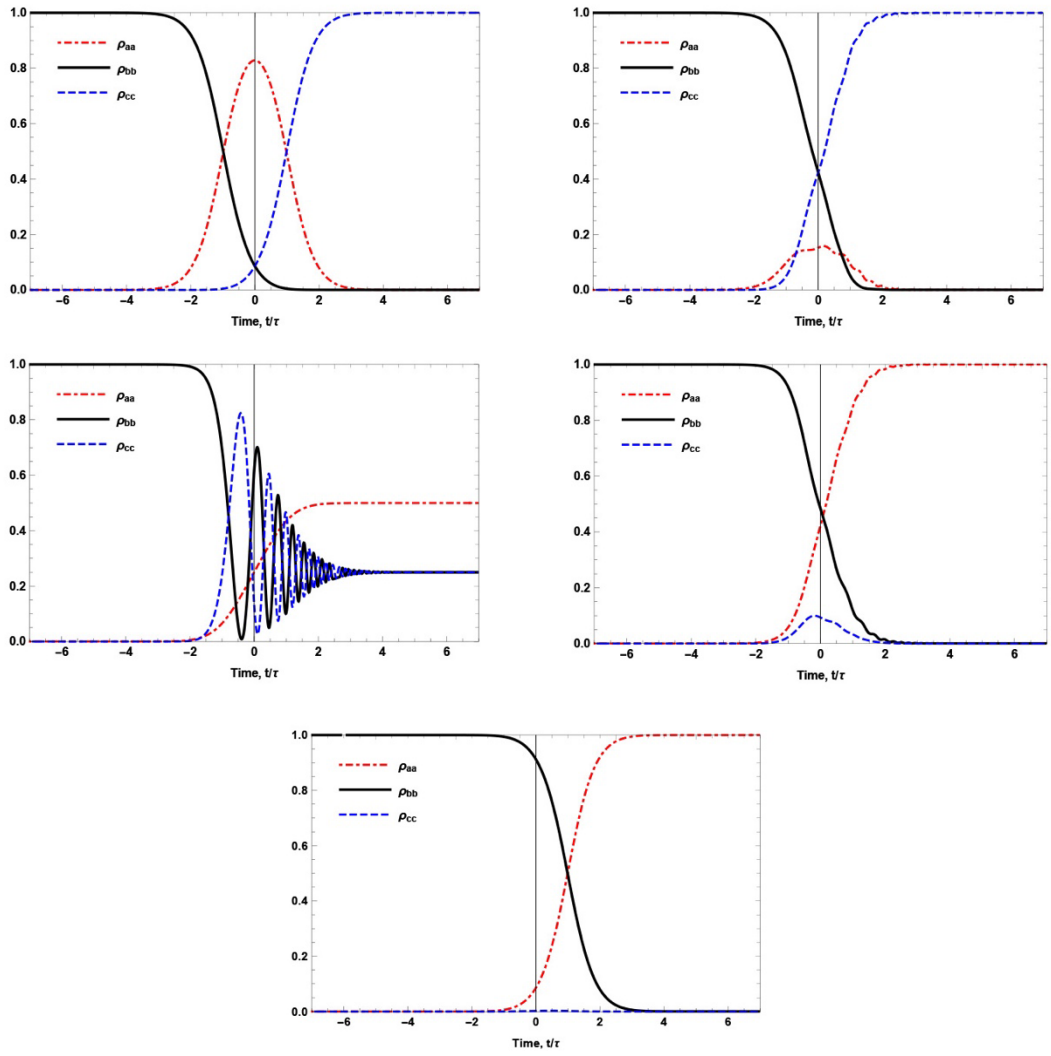


**Figure 5:** The results of simulations demonstrating various excitation of populations are shown for the chirping parameters $\alpha_1 = 6/\tau$, the amplitudes of the pulses are $\Omega_1 = \Omega_2 = 5/\tau$ and $\alpha_2 = -\alpha_1$ with different delay times $\tau_d$: (a) $\tau_d = -\tau$, (b) $\tau_d = -0.25\tau$, (c) $\tau_d = 0$, (d) $\tau_d = 0.25\tau$, $(e)$ $\tau_d = \tau$

For short-duration pulses, the chirping allows to map the spectral content mapped on to temporal distribution.

## 2.4 Role of the Coherent Population Trapping for Chirped Pulses

Let us start with a simple remark. The chirped pulses are efficient for population excitation of two-level atoms, but usually the atoms under consideration have more levels, for example, Rb of Cs atoms have more levels in the ground states because of magnetic sublevels. Thus, it is interesting to see the effect of chirped pulses taking into account that the ground state consists of more than one level (for example two, see Figure 4(A) and the levels are coupled to the excited states by the same optical pulse as shown in Figure 4(B)). In this case, the basis of the so called “dark” and “bright” states are very useful (initially the “dark” and “bright” states are populated equally), and we can see the population dynamics in this case. We can see simple full population transfer as we would expect for a two-level system and the so-called “dark” state is totally decoupled from the field. It means that the coherence between ground states are excited by the chirped pulse as we can see clearly in Figure 4(C).

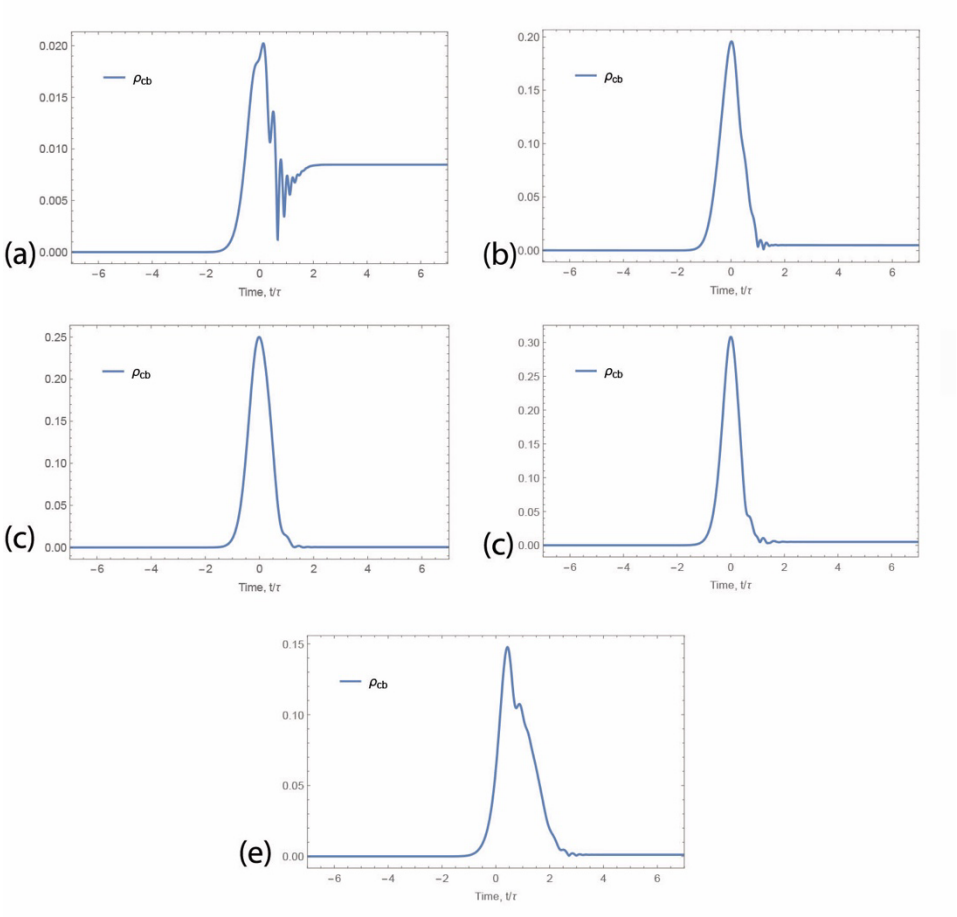


**Figure 6**: The results of simulations demonstrating various excitation of populations are shown for the chirping parameters $\alpha_1 = 6/\tau$, the amplitudes of the pulses are $\Omega_1 = \Omega_2 = 5/\tau$ and $\alpha_2 = -\alpha_1$ with different delay times $\tau_d$: (a) $\tau_d = -\tau$, (b) $\tau_d = -0.25\tau$, (c) $\tau_d = 0$, (d) $\tau_d = 0.25\tau$, (e) $\tau_d = \tau$

We can clearly see that the chirped pulses are providing the efficient ways to manipulate the quantum coherence of ground states and the population of the exciting states. It would be interesting to study how the manipulations depend on the delay time between the chirped pulses and the relaxation rates of the excited states.

Two-level system interacting with chirped pulse. But if two-level system has degenerate ground state, consisting of magnetic sub-levels, for example. It is shown in Figure 4A. Then, we can see that the ground state can be viewed like two states – dark

and bright, and interaction only with bright state. Then due to chirped pulse interaction the population from bright state will be excited to state a, and dark state will stay untouched. But it means that the coherent superposition of state b and c will be excited, as one can see in Figure 4B. In Figure 4aC, the chirped pulse is shown, the pulse interacts with both transitions. Below, we do not take into account these effects, considering the ground states as single levels. The effect is clearly understood, and it can be important for spectroscopy (see details and discussions in [68]).

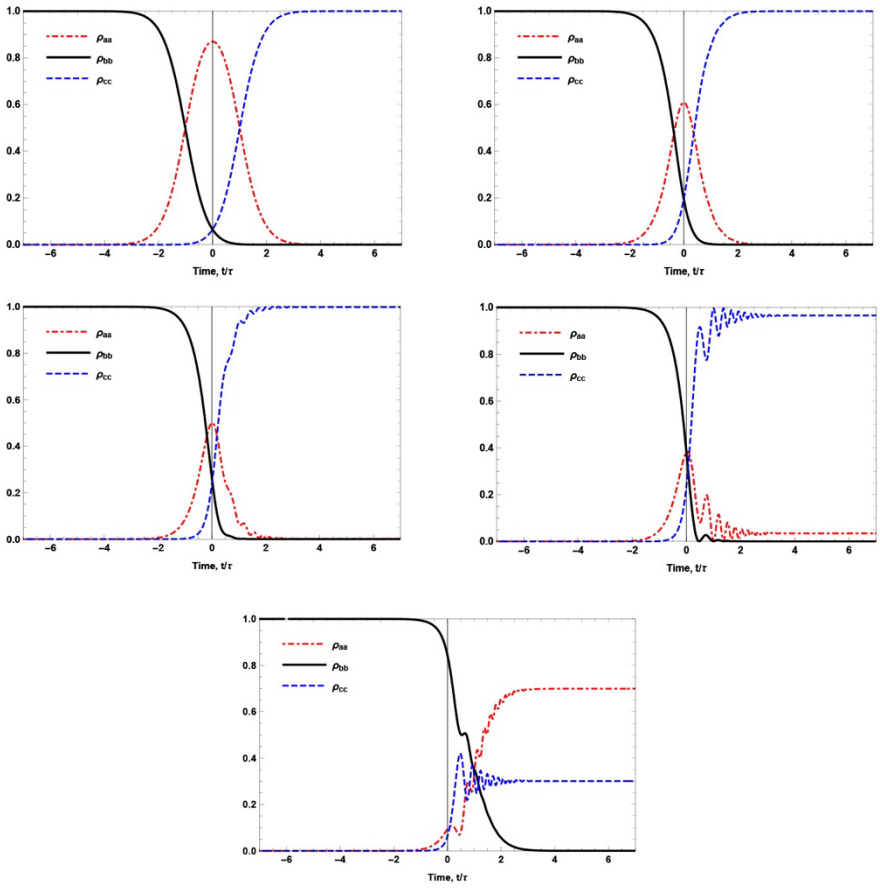


**Figure 7**: The results of simulations demonstrating various excitation of populations are shown for the chirping parameters $\alpha_1 = 6/\tau$, the amplitudes of the pulses are $\Omega_1 = \Omega_2 = 5/\tau$ and $\alpha_2 = \alpha_1$ with different delay times $\tau_d$: (a) $\tau_d = -\tau$, (b) $\tau_d = -0.25\tau$, (c) $\tau_d = 0$, (d) $\tau_d = 0.25\tau$, (e) $\tau_d = \tau$.

## 2.5 Efficient Manipulation of Quantum Coherence and Populations in Atomic and Molecular Media

Next question, what kind of state control can we obtain applying chirped pulses to atomic/molecular systems. We have already seen efficient excitation of the excited states, but it would be instructive to study what kind of manipulations and quantum states can be obtained in three level systems with application to different chirped pulses with appropriate tailoring pulse shapes. For example, we may introduce different chirping and delaying pulses with respect to each other. Here, we see very efficient quantum control of the final states that can be generated by properly tailored pulses. The results are also very robust and tolerant to some extended variation of the input pulses. This can be important if we are able to apply these results in a dense media where the propagation effects are important.

For example, for opposite signs of the chirped pulses, the population transfer occurs, but no coherence is practically excited in the medium (see Figures 5,6). Meanwhile, with the same signs of the chirped pulses, the coherence excited in a broad range of delays together with population transfer (see Figures 7,8). We find out the limit of the delays between pulses for this population transfer.

We see that the change of the sign of chirping allows one to change the destination of the population transfer, namely from the ground state to the excited states. We also demonstrate the various opportunities of inducing various coherences between various states in the quantum systems.

All possibilities demonstrated here are important and have various application for single atoms and molecular manipulations. It is important to study how all these

manipulations can be implemented for a dense media where the propagation effects are important.

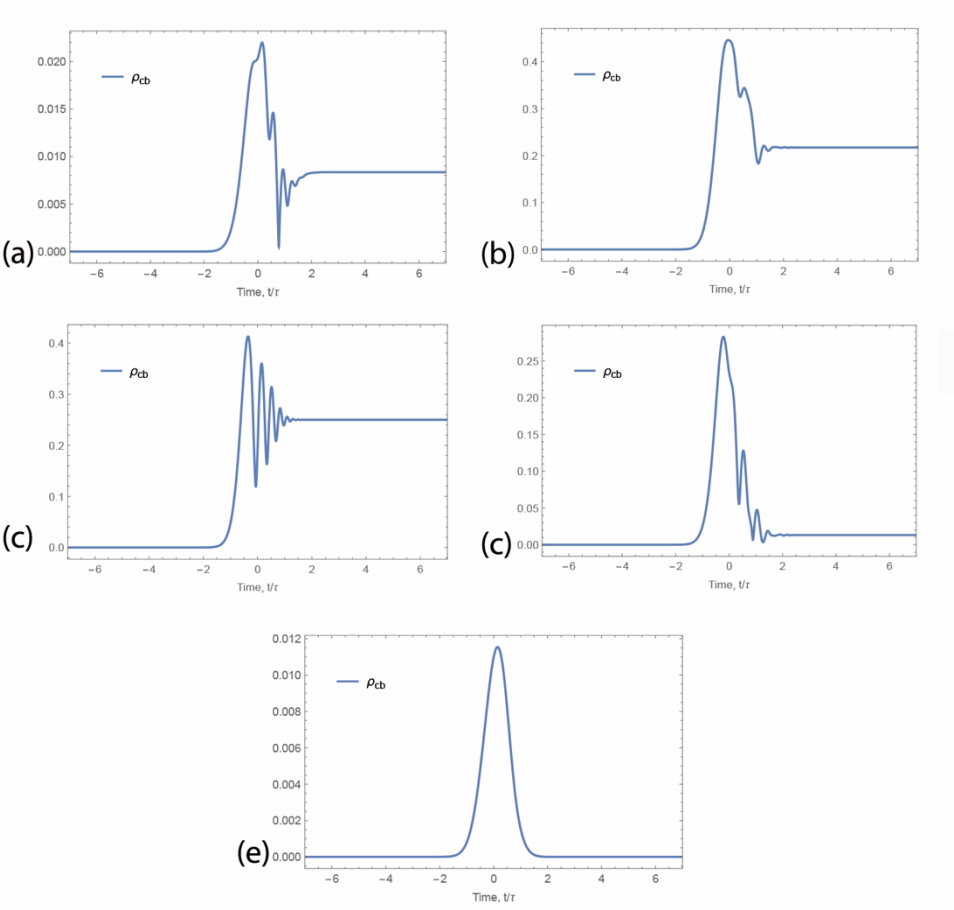


**Figure 6**: The results of simulations demonstrating various excitation of populations are shown for the chirping parameters $\alpha_1 = 6/\tau$, the amplitudes of the pulses are $\Omega_1 = \Omega_2 = 5/\tau$ and $\alpha_2 = -\alpha_1$ with different delay times $\tau_d$: (a) $\tau_d = -\tau$, (b) $\tau_d = -0.25\tau$, (c) $\tau_d = 0$, (d) $\tau_d = 0.25\tau$, (e) $\tau_d = \tau$.

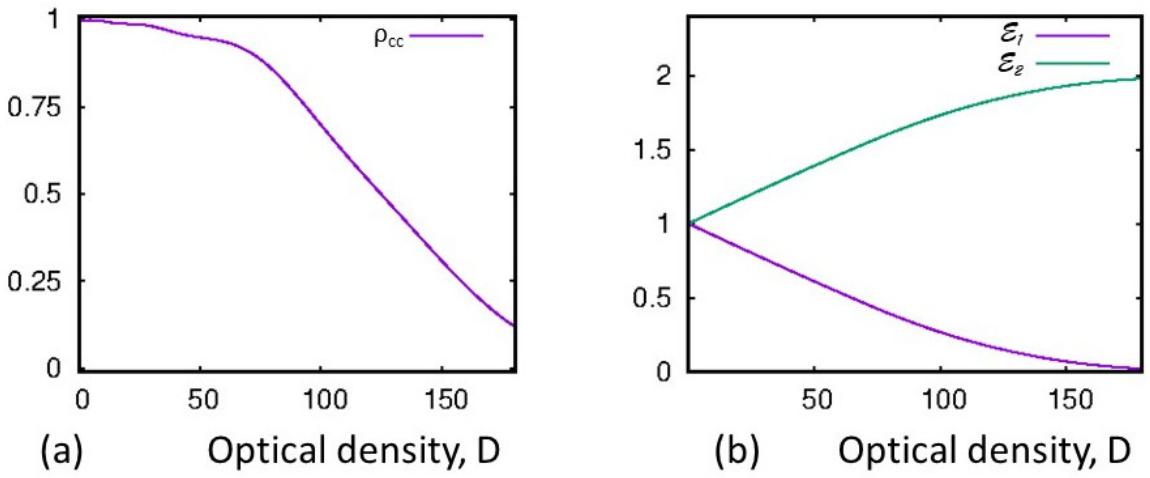


**Figure 7**: Population dynamics vs time are shown using STIRAP. (a) The efficiency of population transfer vs optical density. (b) The energy of the pulses vs optical density.

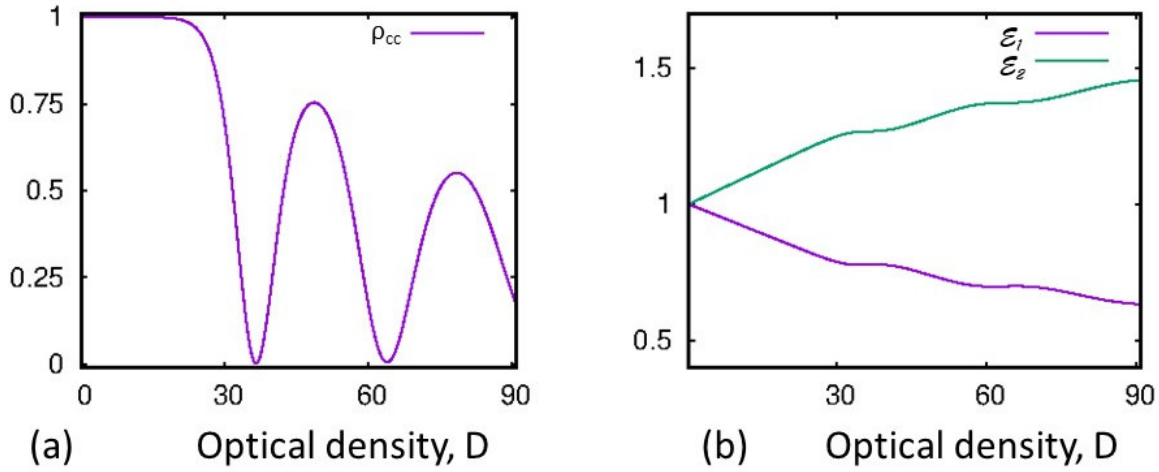


**Figure 8**: Population dynamics vs time is shown using the chirped pulses. (a) The efficiency of population transfer vs optical density. (b) The energy of the pulses vs optical density.

2.6 Propagation Effects for the Adiabatic Pulses

Now we turn to propagation effects. The spatial and temporal evolution of $\Omega_1$ and $\Omega_2$ are given by

$$\left(c\frac{\partial}{\partial z}+\frac{\partial}{\partial t}\right)\Omega_1 = -i\Omega_{a1}^2\rho_{ab} \tag{39.1}$$

$$\left(c\frac{\partial}{\partial z}+\frac{\partial}{\partial t}\right)\Omega_2 = -i\Omega_{a2}^2\rho_{ac} \tag{39.2}$$

where the $\Omega_{a1,2}^2 = c\eta_{1,2}$ are the so-called cooperative frequencies. Using the basis of the "dark" and "bright" states, we can obtain the propagation equation for the effective Rabi frequency $\Omega_e$ as.

$$\left(c\frac{\partial}{\partial z}+\frac{\partial}{\partial t}\right)\Omega_e = -i\Omega_a^2\rho_{aB} \tag{40.0}$$

Let us note that, for the adiabatic optical pulses, the population is in the dark state, $\rho_{DD} \simeq 1$, thus $\rho_{aB} \simeq 0$, (Figure 5) and the effective Rabi frequency does not change during propagation such that $\Omega_e \simeq \text{const}$. Finally we obtain,

$$\left(c\frac{\partial}{\partial z}+\frac{\partial}{\partial t}\right)\left(\frac{|\Omega_1|^2}{\Omega_{1a}^2}+\frac{|\Omega_2|^2}{\Omega_{2a}^2}\right)+\frac{\partial}{\partial t}\rho_{aa} = 0 \tag{41.0}$$

it has a simple physical meaning, and can be re-written in the form of

$$\left(c\frac{\partial}{\partial z}+\frac{\partial}{\partial t}\right)(\mathcal{N}_1+\mathcal{N}_2)+N\frac{\partial}{\partial t}\rho_{aa} = 0 \tag{42.0}$$

where $\mathcal{N}_1 = \frac{|E_1|^2}{4\pi\hbar\omega_1}$ and $\mathcal{N}_2 = \frac{|E_2|^2}{4\pi\hbar\omega_2}$ are the photon density of the laser beams, and N is the molecular density. The Eq. (42.0) can be interpreted as the conservation of the photon flux and the population in the excited atomic state. Meanwhile, the sum of $\mathcal{N}_1$ and $\mathcal{N}_2$ is conserved, the number of photons in pulses are related to the population in the levels b and c, namely

$$\left(c\frac{\partial}{\partial z}+\frac{\partial}{\partial t}\right)\mathcal{N}_1 = N\frac{\partial}{\partial t}\rho_{bb} \tag{43.1}$$

$$\left(c\frac{\partial}{\partial z}+\frac{\partial}{\partial t}\right)\mathcal{N}_2 = N\frac{\partial}{\partial t}\rho_{cc} \tag{43.2}$$

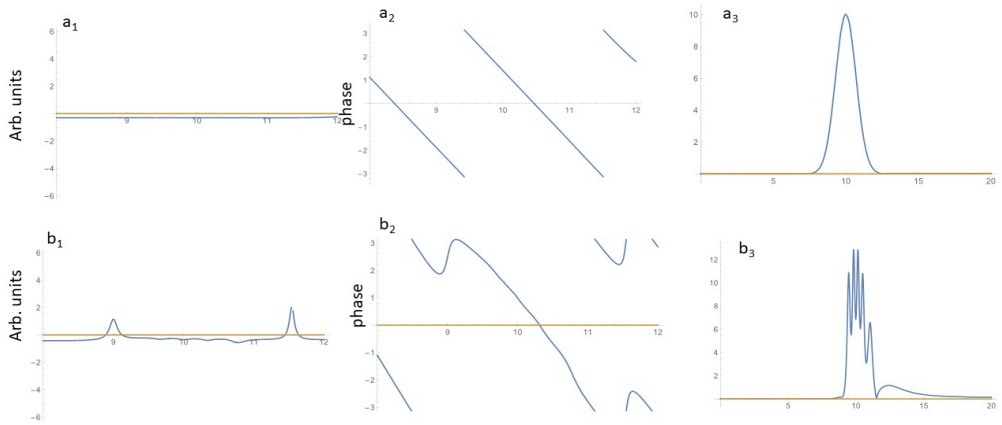


**Figure 9**: The instantaneous frequency $(a_1\ and\ b_1)\ \omega(t) = \partial\Phi(t)/\partial t$, and the time dependence of the phase of the electromagnetic fields $\Phi(t)$ $(a_2\ and\ b_2)$ and the pulse shape $|\Omega(t)|$ $(a_3 and\ b_3)$ for different optical density: plots $a_1, a_2, and\ a_3$ correspond to the optical density $D = 0$, plots $b_1, b_2, and\ b_3$ to the optical density $D = 20$.

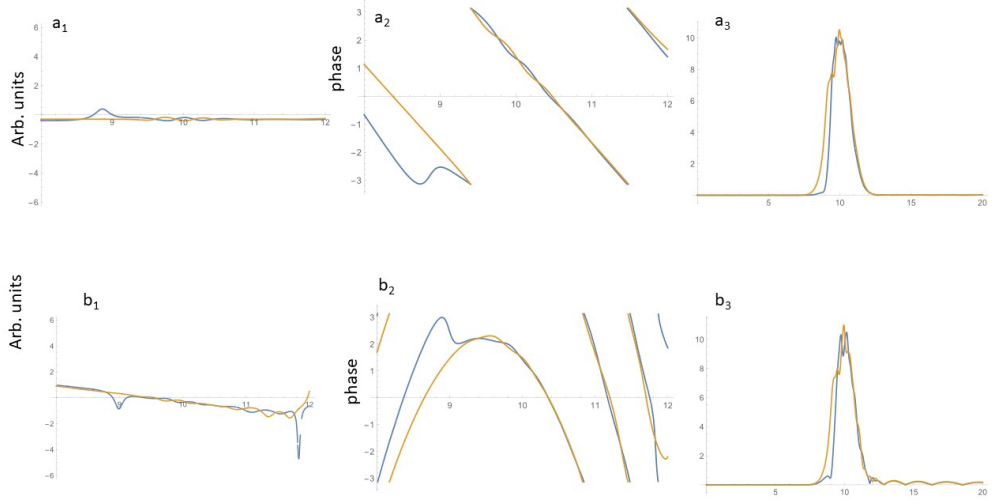


**Figure 10**: The instantaneous frequency and the time dependence of the phase of the electromagnetic fields for different optical density: plots $a_1\ and\ a_2$ correspond to the optical density 0, plots $b_1 and\ b_2$ to the optical density 0.

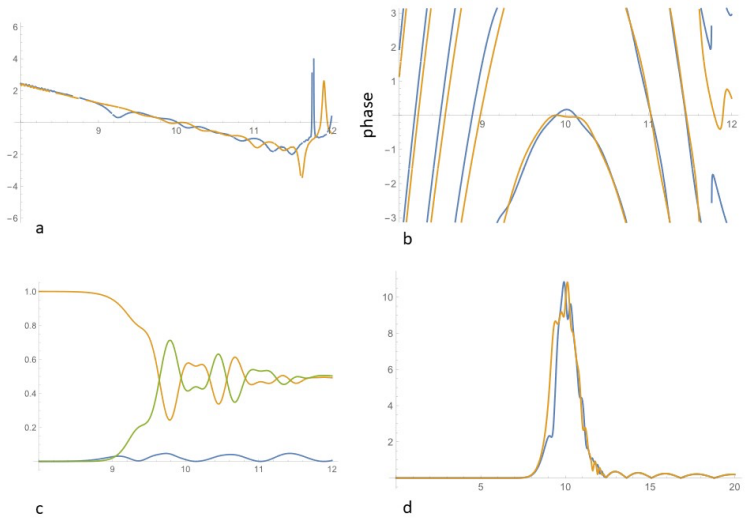


**Figure 11:** The instantaneous frequency and the time dependence of the phase of the electromagnetic fields for different optical density: plots

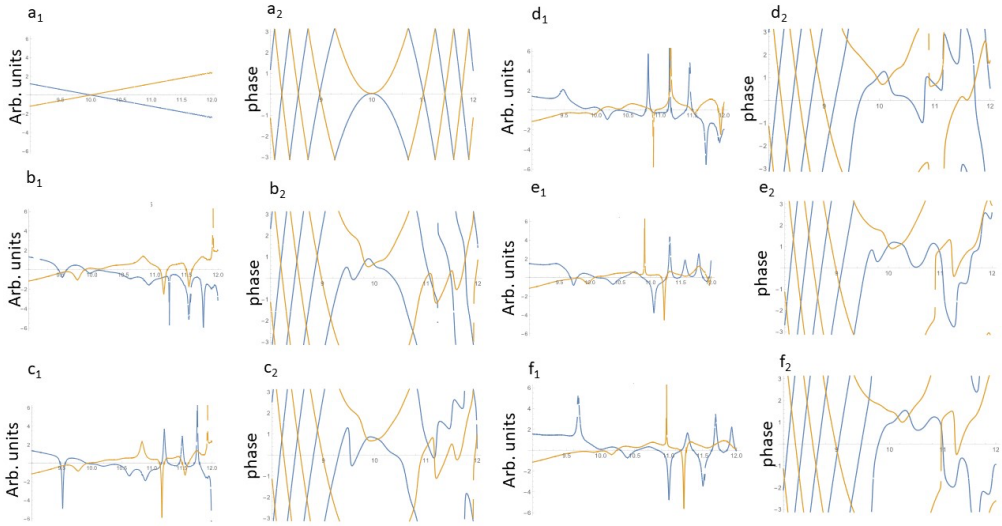


**Figure 12**: The instantaneous frequency and the time dependence of the phase of the electromagnetic fields for different optical density: plots $a_1$ and $a_2$ correspond to the optical density 0, plots $b_1$ and $b_2$ to the optical density 0, plots $c_1$and $c_2$ to the optical density 0, plots $d_1$ and $d_2$ to the optical density 0, plots $e_1$ and $e_2$ to the optical density 0, plots $f_1$ and $f_2$ to the optical density 0.

It is important for applications to study the effect of control of quantum systems along the laser pulses propagating through the media. For this task, we have solved together with propagation Eqs. (39.1, 39.2) and the density matrix equations Eqs. (31.1-32.3) together.

We perform simulations and the results of simulations are shown in Figures 9, 10. As expected, the laser pulses experience strong changes during propagation through the resonant media. Nevertheless, one can also see that the efficient Rabi frequency $\Omega_e$ does not practically change during propagation as it follows from Eq.(36.3) for adiabatic optical pulses. The relative pulse energies can be characterized by

$$\mathcal{E}_{1,2} = \frac{\int_{-\infty}^{\infty} |\Omega_{1,2}(t,z)|^2 dt}{\int_{-\infty}^{\infty} |\Omega_{1,2}(t,z=0)|^2 dt} \quad (44.0)$$

the dependence of relative charge of pulse energies are shown in Figure 6,7.

## 2.7 Acknowledgements

We thank Adam Voight, Marshall Rogers, Konstantin Dorman and Stephen Schiller for fruitful discussions, comments and suggestions. C.R. and Y.R. are grateful for the support by Dr. Glen Perram and the 2021 AFOSR Summer Faculty Fellowship Program at AFIT. We also gratefully acknowledge the support from the University of North Texas Global Venture Fund, and from the College of Science Collaborator's Seed Grant at the University of North Texas. A.P. is thankful for the AFOSR grant.

# CHAPTER 3

# TUNABLE MASERS[1]

## 3.1 Introduction

The maser (microwave amplification by stimulated emission of radiation), the coherent source of the microwave radiation similar to the laser, was demonstrated in 1954 [1]. However, unlike lasers [2], the masers are much less widely used because in order to function, they must be cooled to temperatures close to absolute zero. In 2012, it was demonstrated that a maser could operate at room temperature using the organic molecule pentacene. However, it only produced short pulses of maser radiation. For continuous operation of the maser, the crystal would likely have melted [3]. Only recently, it was reported that a new maser is created that operates continuously [4].

Meanwhile, we have to underline here that the maser technology being used where sensitive detection of microwave radiation is essential. The masers could be used in a range of applications such as medical imaging and airport security scanning. They have more traditionally been used in deep space communication and radio astronomy. As well as medical imaging and airport security scanning, masers could play a pivotal role in improving sensors to remotely detect bombs, new technology for quantum computers, and might even improve space communication methods to potentially find life on other planets. Thus, the development tunable maser working at room temperature is very important.

[1] This chapter is reproduced in its entirely from C. D. Roy, Z. Brankovic, and Y. Rostovtsev, "Weakly Aligned Molecules: From Molecular Detectors to Room Temperature Tunable Masers," Journal of Physics: Conference Series 2249 (1), 012001 (2022), with permission from IOP Publishing.

On the other hand, to detect molecular gas dispersion or absorption or to create population inversion in molecular levels at room temperature is difficult for rotational frequencies because the population difference is very low at room temperature and probability to absorb photon is very low. Indeed, the probability for photon being absorbed is given by

$$P_{abs} = 1 - \exp\left[-\frac{\omega_{ab}\wp_{ab}^2 N_0 L}{c\hbar\Gamma_{ab}} n_{ab}\right] \quad (45.0)$$

where $\omega_{ab}$ is the frequency of transition, $\wp_{ab}$ is the dipole moment, $\Gamma_{ab}$ is the width of transition, $N_0$ is the gas density, and $n_{ab}$ is the population difference between corresponding levels. It is clear that low frequency $\omega_{ab}$ and small $n_{ab}$ results in low absorption probability. But it would be desirable to enhance the probability of absorption for individual molecules to 100 %, so each molecule can absorb one photon. Then, this can be extremely useful to reach maximal absorption for gas detectors as well as creation of population inversion in a molecular gas for the maser operation.

In this chapter, we show that developing techniques to control and to manipulate the populations in the rotational molecular levels can enhance the sensitivity of gas detection, and also it can open possibilities of creation population inversion that can be used for developing masers working at room temperature.

Applying a dc electric field aligns molecules along the field, and modifies the rotational energy levels of molecules [5, 6] (see Figure 15(a)). Aligned molecules can be viewed as simple pendulums that have the energy structure of a simple harmonic oscillator (see Figure 15(a)). Even a small electric field produces the weak alignment that can be take advantage for development various techniques of quantum control of rotational molecular states. The control is based on an adiabatically changing electric

field that interacts with the rotational structure of the molecules with dipole moments. In particular, these new techniques are important for developing gas masers at room temperature as well as the developing of new gas sensors with higher selectivity and sensitivity [7, 8]. There are several physical mechanisms to change absorption that are related to the so-called quantum coherent effects. Quantum coherence effects, such as coherent population trapping [9] and electromagnetically induced transparency (EIT) [10, 11, 12], have been the focus of a broad range of research activity for the past two decades since they drastically change the optical properties of the media. In EIT, for example, absorption practically vanishes in both the CW and the pulsed regime [11]. A medium with an excited quantum coherence, phaseonium [10], can be used to make an ultra-dispersive prism [13] which will have several orders of magnitude greater angular spectral dispersion compared to a conventional one [14, 16-19]. The importance and success of proper quantum engineering was demonstrated, in particular, for the pulse shaping in coherent raman spectroscopy [20] that allows researchers to improve sensitivity. Here, we propose a new approach that results in the enhancement of the population difference between corresponding molecular levels and reaches the theoretical maximum of absorption.

The new approach to the problem is based on introducing mechanism based on an adiabatically changing electric field interacting with the rotational structure of the molecules with dipole moments. Normally the gases do not absorb radiation if optical density is very small. Contrary, using this approach, every gas molecule absorbs a photon. This can be reached by using an adiabatically changing electric field that is sweeping the resonant frequency through the frequency of the ac probe field resulting in

complete population transfer in the molecular system. Together with the change of photon numbers, the phase change of the probe field occurs. Both changes can be used as signals for gas sensing. Using proper tailoring of the adiabatically changing electric field allows researchers to resonantly enhance the sensor signal reaching the theoretical limit.

3.2 Interaction with Chirping Adiabatic Pulses

Let us consider the interaction of the adiabatically changing fields with a two-level system. For the two-level atom, the Hamiltonian is given by

$$\hat{\mathrm{H}} = \hbar\Delta|\mathrm{a}\rangle\langle\mathrm{a}| + \hbar\Omega(|\mathrm{a}\rangle\langle\mathrm{b}| + |\mathrm{b}\rangle\langle\mathrm{a}|) \tag{46.0}$$

where $\mathrm{a}$ and $\mathrm{b}$ are the excited and ground levels of the atom, $\Delta = \omega_{\mathrm{ab}} - \omega$ is the detuning between frequency of the field $\omega$ and the resonance frequency of the transition $\omega_{\mathrm{ab}}$, $\Omega$ is the coupling due to interaction with adiabatically changing field. The eigenvalues are

$$\lambda_{\pm} = \omega_{\pm} = \frac{\Delta}{2} \pm \sqrt{\left(\frac{\Delta}{2}\right)^2 + \Omega^2} \tag{47.0}$$

and eigenvectors are given by

$$|\pm\rangle = \frac{\omega_{\pm}|\mathrm{a}\rangle + \Omega|\mathrm{b}\rangle}{\sqrt{\omega_{\pm}^2 + \Omega^2}} \tag{48.0}$$

Let us note here that for $\Omega = 0$ and $\Delta > 0$: $\omega_+ = \Delta, |+\rangle = |\mathrm{a}\rangle$ and $\omega_- = 0, |-\rangle = |\mathrm{b}\rangle$, and for $\Omega = 0$ and $\Delta < 0$: $\omega_+ = 0, |+\rangle = |\mathrm{b}\rangle$ and $\omega_- = \Delta, |-\rangle = |\mathrm{a}\rangle$. For $\Omega \neq 0$, adiabatically changing $\Delta$ from $-\infty$ to $+\infty$ leads to adiabatical changes $\omega_{\pm} \rightarrow \omega_{\mp}$ and $|\pm\rangle \rightarrow |\mp\rangle$, as

$$\omega_+(\Delta) = \begin{cases} 0\,, \Delta \rightarrow -\infty \\ \Delta\,, \Delta \rightarrow +\infty \end{cases} \text{ and } |+\rangle(\Delta) = \begin{cases} |\mathrm{b}\rangle, \Delta \rightarrow -\infty \\ |\mathrm{a}\rangle, \Delta \rightarrow +\infty \end{cases} \tag{49.1}$$

$$\omega_-(\Delta) = \begin{cases} \Delta\,, \Delta \rightarrow -\infty \\ 0\,, \Delta \rightarrow +\infty \end{cases} \text{ and } |-\rangle(\Delta) = \begin{cases} |\mathrm{a}\rangle, \Delta \rightarrow -\infty \\ |\mathrm{b}\rangle, \Delta \rightarrow +\infty \end{cases} \tag{49.2}$$

and the states $|\mathrm{a}\rangle$ and $|\mathrm{b}\rangle$ can be expressed in terms of $|\pm\rangle$ states as.

$$|\mathrm{a}\rangle = \frac{\sqrt{\omega_+^2+\Omega^2}\left|+\right\rangle-\sqrt{\omega_-^2+\Omega^2}\left|-\right\rangle}{2\sqrt{\left(\frac{\Delta}{2}\right)^2+\Omega^2}} \text{ and } |\mathrm{b}\rangle = \frac{-\omega_-\sqrt{\omega_+^2+\Omega^2}\left|+\right\rangle+\omega_+\sqrt{\omega_-^2+\Omega^2}\left|-\right\rangle}{2\Omega\sqrt{\left(\frac{\Delta}{2}\right)^2+\Omega^2}} \qquad (50.0)$$

Then, an arbitrary state $|\psi_\mathrm{i}\rangle = \mathrm{A}|\mathrm{a}\rangle + \mathrm{B}|\mathrm{b}\rangle$ changes into $\left|\psi_\mathrm{f}\right\rangle = \mathrm{B}e^{\mathrm{i}\phi_\mathrm{a}}\left|\mathrm{a}\right\rangle + \mathrm{A}e^{\mathrm{i}\phi_\mathrm{b}}|\mathrm{b}\rangle$, performing swap the populations in the states. It is a remarkable because it can lead to the maximal absorption on one hand, and to creation of population inversion on the other. Below there are applications of this swap of populations to the gas sensing and to the maser operation.

3.3 Theoretical Model

For simplicity and to understand essential physics, we consider molecules with electric dipole moments $\vec{\wp}$, and the Hamiltonian in the dc electric field $\vec{\mathcal{E}}_0$ is given by.

$$\hat{\mathrm{H}} = \mathrm{B}\hat{\mathrm{J}}_\mathrm{z}^2 - \vec{\wp}\cdot\vec{\mathcal{E}}_0 \qquad (51.0)$$

Here, we can view symmetric molecules as simple rotators (see Figure 15(a)) to simplify our consideration [21] ($\mathrm{B} = \hbar^2/2\mathrm{I}$, $\mathrm{I}$ is the moment of inertia).

The first excited rotational states are split in the dc electric field due to Stark effect (see Figure 1(b,c)), and this energy splitting depends on $\mathcal{E}_0$.

$$\frac{2\mathrm{I}(\mathrm{E}_2-\mathrm{E}_1)}{\hbar^2} = \mathrm{F}\left(\frac{2\wp\mathrm{I}\mathcal{E}_0}{\hbar^2}\right) \qquad (52.0)$$

The splitting can be tuned to any frequency $\omega_0 = \frac{(\mathrm{E}_2-\mathrm{E}_1)}{\hbar}$, and the transition can be used for maser operation and for spectroscopy as well. The strong (dc or slowly varying) electric field control the population and the splitting between levels, and the ac electric field orthogonal to the dc field is tuned to the resonance with the molecule's transitions. To pump maser the ac and maser and. pump field is used. Then, for maser operation

and spectroscopy, the maser field and the probe field are ac fields with frequencies from RF to microwave range. The ac pump probe fields $\mathcal{E}_s$ can be created by the high finesse resonance circuits or high finesse microwave cavities. The equation for the Rabi frequency $\Omega_s = \wp\mathcal{E}_s/\hbar$ is given by

$$\dot{\Omega}_s = -i(\omega_0 - \omega_s)\Omega_s + i\Omega_a^2\rho_{ab} \tag{53.0}$$

$$\frac{\partial\rho}{\partial t} = \frac{i}{\hbar}[\rho, H] - \hat{\Gamma}[\rho] \tag{54.0}$$

where $\omega_s$ is the frequency of the resonance circuit, $\Omega_a^2 = \frac{2\pi\omega_0\wp^2 N}{\hbar}$ is the cooperative frequency, and $\rho_{ab}$ is the molecular coherence between the molecular states involved, $\rho_{ab}$ is the element of the density matrix $\rho$. Taking into account relaxation in all processes described above is very important. For this purpose, we use the Liouville-von Neumann equation for the density matrix to describe the time evolution of the molecules. The decoherence of the individual three-level atomic system is taken into account using Lindblad super operator formalism [22]. where $\hat{\Gamma}[\rho]$ is the relaxation matrix for all components of the density matrix $\rho$. The set of density matrix equations are given by

$$\dot{\rho}_{ab} = -(\Gamma_{ab} + i\Delta)\rho_{ab} + in_{ab}\Omega_s \tag{55.1}$$

$$\dot{\rho}_{bb} = i(\rho_{ba}\Omega_s - \Omega_s^*\rho_{ab}) \tag{55.2}$$

$$\dot{\rho}_{aa} = i(\rho_{ab}\Omega_s^* - \Omega_s\rho_{ba}) \tag{55.3}$$

where $n_{ab} = \rho_{aa} - \rho_{bb}$, and $\Delta = \omega_{ab}(\Omega_0) - \omega_0$.

The modification of the energy structure leads also to redistribution of population in the rotational levels. Namely, the population difference between levels $\tilde{m} = 1$and $\tilde{m} = 2$ (see in Figure 15(d) and even more clear see Figure 16(A), (B), (C)) is given by

$$N_2 - N_1 = \frac{\hbar^2 N_0}{2Ik_B TZ} F\left(\frac{2\wp I\mathcal{E}_0}{\hbar^2}\right), \text{where } Z = \sum_{\tilde{m}=0}^{\infty} e^{-\frac{E_{\tilde{m}}}{k_B T}} \tag{56.0}$$

where $k_B$ is the Boltzmann constant, $T$ is the room temperature, and $N_0$ is the molecular gas density. The population distribution for case of the electric field strong enough as shown in Figure 16(C) will transfer to the same population difference in Figure 16(B) with adiabatic change of the electric field $\mathcal{E}_0$. We can see that this is similar to the magnetic cooling with the adiabatically changing magnetic field [23-25]. In our approach, we use a molecular gas with weakly aligned molecules in a dc electric field.

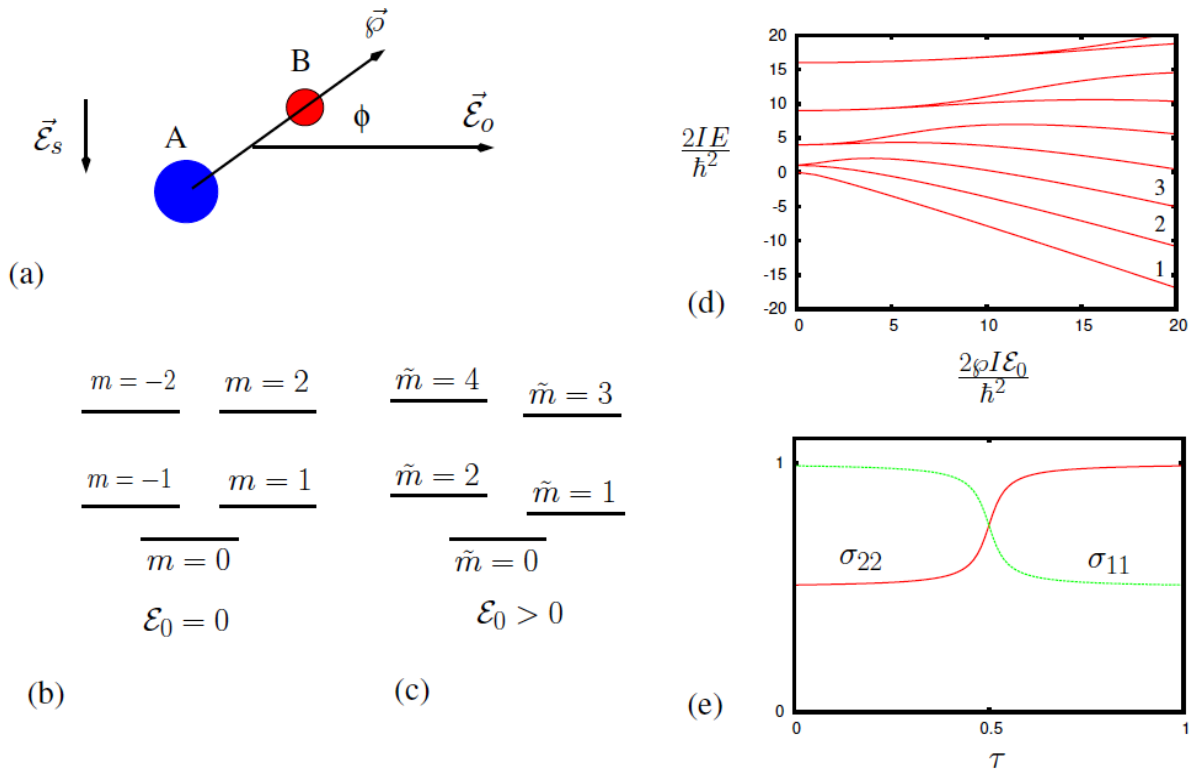


**Figure 13:** (a) Molecular rotator with electric dipole $\vec{\wp}$, where $\phi$ is the angle of rotation with respect to the electric field $\mathcal{E}_0$, and the ac electric field $\vec{\mathcal{E}}_s$ orthogonal to the dc field that is tuned to the resonance with the molecules transitions; (b) the energy structure of the molecular rotator with no electric field ($\mathcal{E}_0 = 0$); (c) the energy structure of the molecular rotator with electric field ($\mathcal{E}_0 > 0$); (d) Molecular energy $2IE_{\tilde{m}}/\hbar^2$ dependence on $2I\wp\mathcal{E}_0/\hbar^2$. The numbers 1, 2, and 3 correspond to the states with $\tilde{m} = 0$, $\tilde{m} = 1$, and $\tilde{m} = 2$ correspondingly. (e) Dependence of the population in levels $\tilde{m} = 1$ and $\tilde{m} = 2$ on time $\tau$ .

For complete alignment, a much stronger dc electric (or strong ac electric fields) has to be applied. Indeed, for the total molecular alignment, we need the energy difference between molecular levels be larger than the thermal energy, i.e.,

$$\hbar\omega_{\mathrm{E}} \gg \mathrm{k_B T} \tag{57.0}$$

where $\mathrm{k_B}$ is the Boltzman constant, and

$$\wp\mathcal{E}_0 \gg \left(\frac{\mathrm{k_B T}}{\hbar \mathrm{B}}\right)^2 \hbar \mathrm{B} \tag{58.0}$$

that gives a simple estimation of the dc electric field to be of the order of $\mathcal{E}_0 \simeq 100\ \mathrm{MV/cm}$. We consider the very weak alignment of molecules in the dc field which leads to the resonance with the ac electric field. For the weak alignment, we need to have the dc electric field be sufficiently strong that the coupling is comparable with the rotational splitting, i.e.

$$\wp\mathcal{E}_0 \simeq \hbar \mathrm{B} \tag{59.0}$$

that gives the field to be of the order of $\mathcal{E}_0 \simeq 10$ kV/cm. Our estimations have been made for two frequencies: $\omega_0 = (2\pi)5$ MHz, corresponding to be of the order of $\mathcal{E}_0 \simeq 1$ kV/cm and $\omega_0 = (2\pi)10$ GHz to be if the order of $\mathcal{E}_0 \simeq 30$ kV/cm.

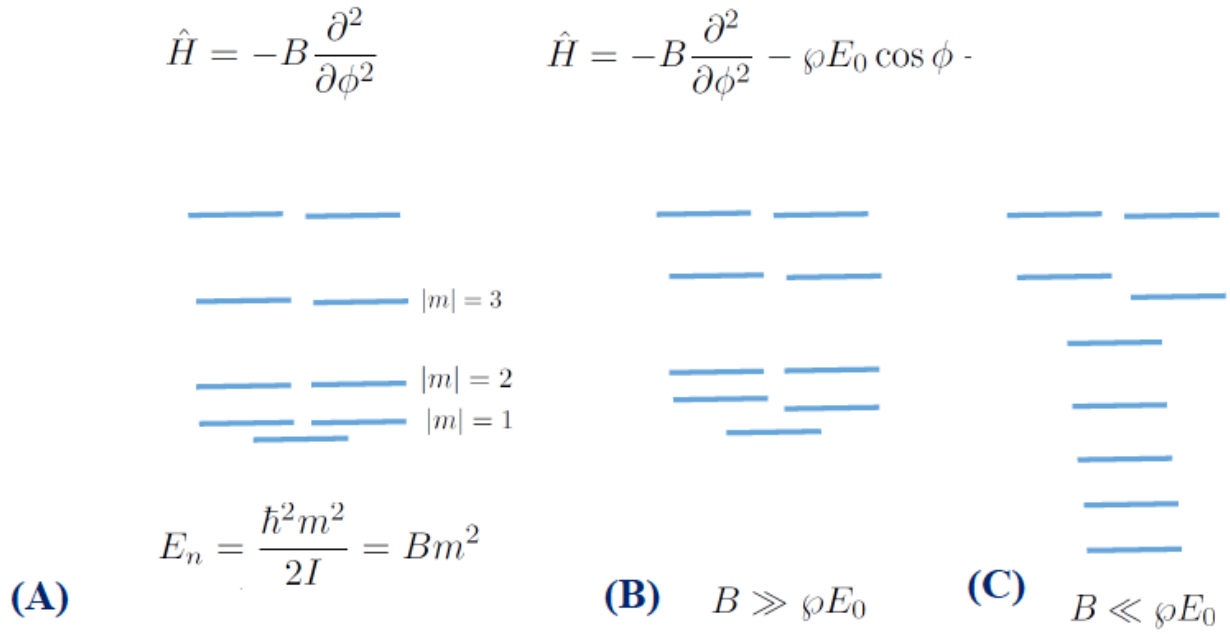


Figure 16: Molecular level structure in the different dc electric fields. (A) $\mathcal{E}_0 = 0$, no dc field, level structure of rotator; (B) $\mathcal{E}_0$ is weak ($B \gg \wp\mathcal{E}_0$), one can see small splitting of the low levels of rotator; (C) $\mathcal{E}_0$ is strong ($B \ll \wp\mathcal{E}_0$), one can see that the low levels of rotator look similar to the levels of the simple harmonic oscillator (see Eq. (15) and Eq. (16)).

Applying a dc electric field modifies the rotational energy levels of molecules (see Figure 15(b, c)), The states $|\widetilde{\mathrm{m}}\rangle$ in the dc electric field with the rotational states $|\mathrm{m}\rangle$ (without electric field) are related as.

$$|\tilde{0}\rangle \rightarrow |\mathrm{m} = 0\rangle, \text{for } \mathrm{m} > 0, |\widetilde{\mathrm{m}} = 2|\mathrm{m}| - 1, 2|\mathrm{m}|\rangle \rightarrow |\pm|\mathrm{m}|\rangle$$

The energy modification can be easily understood by naively considering aligned molecules in the dc electric field [5, 6] (see Figure 16). Aligned molecules can be viewed as simple pendulums. For levels with low energy excitation, they have the

energy structure of a simple harmonic oscillator (see Figure 15(a)). For higher excitation levels, the molecules retain rotational structure.

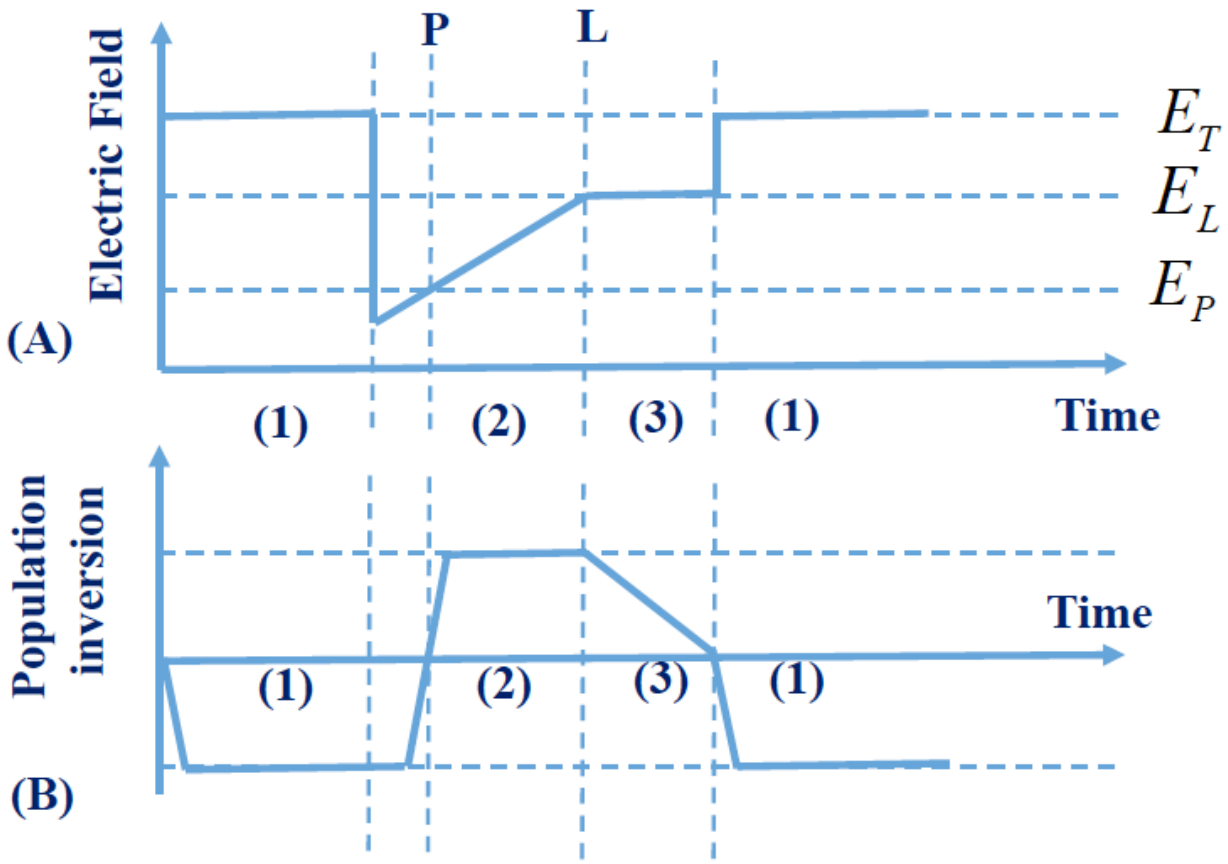


**Figure 14:** Time dependence of the adiabatically changing strong electric field (arbitrary units) $\mathcal{E}_0$ shown in (A). The corresponding population inversion between corresponding levels (arbitrary units) is shown in (B). Different time periods corresponds different phases of molecules in the cavity. (1) - the thermal pumping; (2) - adiabatic change of electric field to produce population inversion between corresponding levels due to some strong field (as shown in Figure 1(e)); (3) - reaching the resonance with maser transition, microwave amplification, depleting all population inversion and then returning to the pumping stage (1).

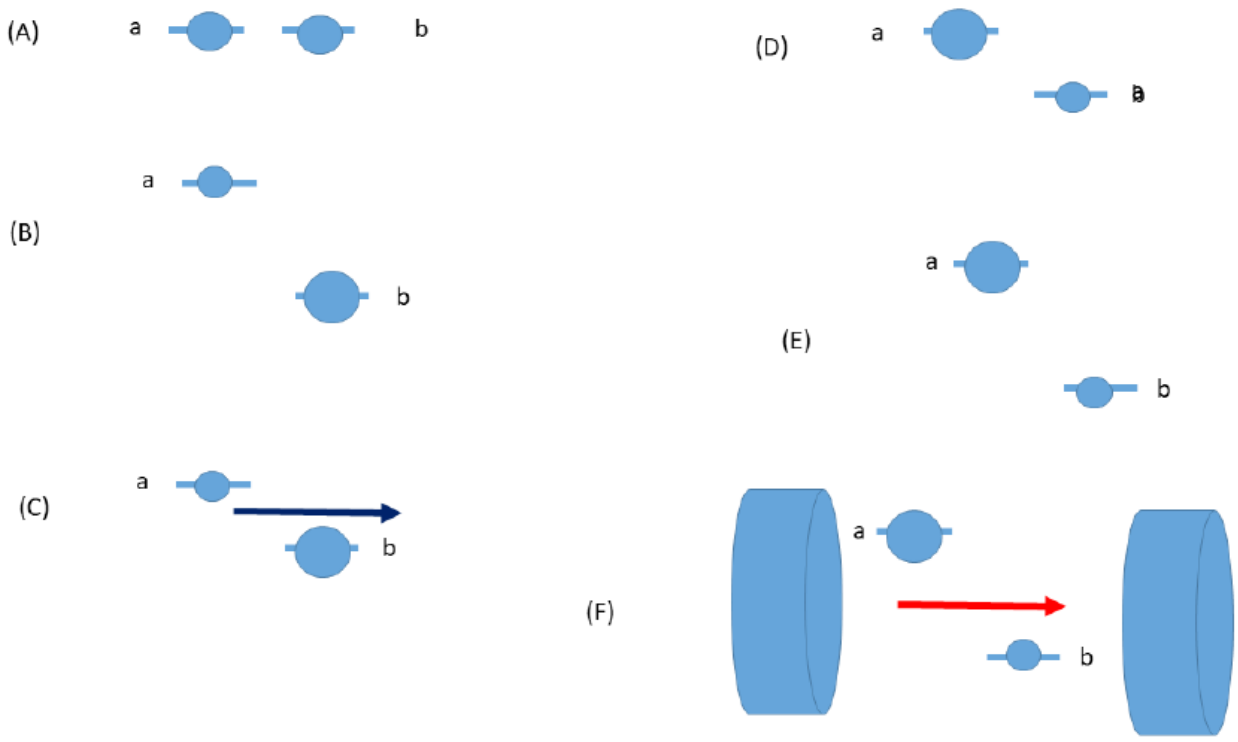


**Figure 15:** Plot shows all stages of population preparation for maser action. (A) Two selected levels from the levels of the molecular rotator that are chosen for serve as a maser transition; (B) Applying a dc field that splits levels, and it creates population difference by thermal equilibrium at room temperature; (C) The splitting tuned to be in resonance with low frequency field to swap population between levels; (D) The swap of population occurs between levels *a* and *b*; (E) The transition is tuned by adiabatic field to the maser cavity frequency; (F) The molecular population inverted levels tuned to cavity frequency and in the cavity produce maser radiation.

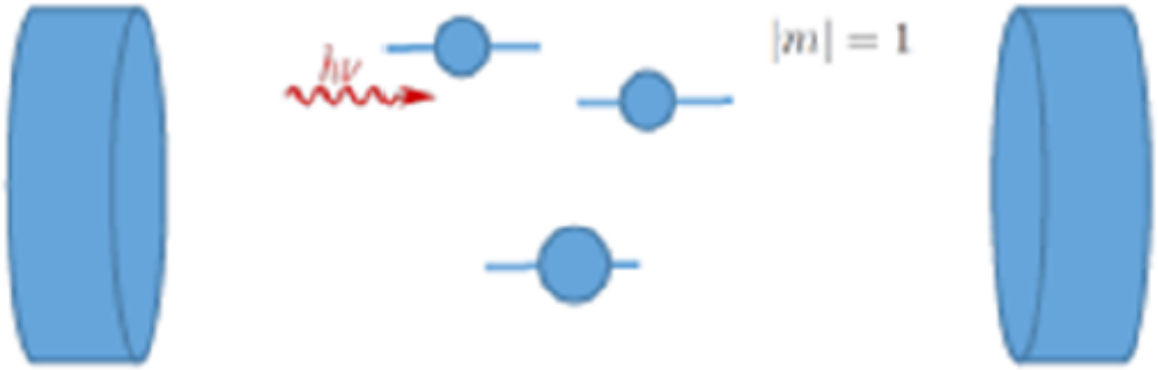


**Figure 16:** It is schematically shown molecular levels of interests (more molecular levels can be seen in Figure 1) with some populations and resonant microwave radiation in the microwave cavity.

The dependance of the molecular energy $\frac{2IE}{\hbar^2}$ on the $\frac{2I\wp\mathcal{E}_0}{\hbar^2}$ is shown in Figure 15(d). It shows that for the larger fields $\wp\mathcal{E}_0 \gg \frac{\hbar^2}{I}$, the electric dipole under the presence of the electric field looks like a simple harmonic oscillator, with the Hamiltonian given by

$$\hat{H} = -\frac{\hbar^2}{2I}\frac{\partial^2}{\partial\phi^2} + \frac{I\omega_E^2}{2}\phi^2 - \wp\mathcal{E}_0 \tag{60.0}$$

where $\omega_E^2 = \frac{\wp\mathcal{E}_0}{I}$. As can be seen in Figure 15(b), the ground and lower states have energies

$$E_{\tilde{m}} \simeq -\wp\mathcal{E}_0 + \hbar\omega_E\left(\tilde{m} + \frac{1}{2}\right) \tag{61.0}$$

Meanwhile, for larger $\tilde{m}$ such that $\frac{\hbar^2}{2I}\tilde{m}^2 \gg \wp\mathcal{E}_0$, the fast molecular rotation completely averages out the effect of the dc electric field, and the molecular energy is $E_{\tilde{m}} \simeq \frac{\hbar^2}{2I}\tilde{m}^2$. One can see that changes in Figure 2 where the molecular level structure is shown in

the different dc electric fields. (A) $\mathcal{E}_0 = 0$, no dc field, level structure of rotator; (B) $\mathcal{E}_0$ is weak ($\mathrm{B} \gg \wp\mathcal{E}_0$), one can see small splitting of the low levels of rotator; (C) $\mathcal{E}_0$ is strong ($\mathrm{B} \ll \wp\mathcal{E}_0$), one can see that the low levels of rotator look similar to the levels of the simple harmonic oscillator (see Eqs. 60.0, 61.0). Then, the proposed maser scheme works in the following stages (see Figures 17 and 18). First, we can choose the levels that can be used for our maser transition (see Figure 18(A)), these can be levels with $|\mathrm{m}| = 1$ (see Figure 15). Maser starts at the stage (1), at some relatively strong dc electric field $\mathcal{E}_0$ that causes the weak alignment of molecules. The maser levels a and b are split (see Figure 18(B)). The molecules have the corresponding thermal distribution between molecular levels. Then, the electric field $\mathcal{E}_0$ changes to the vicinity of the electric field $\mathcal{E}_\mathrm{P}$ that corresponds coherent pump field (see Figure 18(C)). Time dependence of the adiabatically changing strong electric field (arbitrary units) $\mathcal{E}_0$ shown in Figure 17(A). The corresponding population inversion between corresponding levels (arbitrary units) is shown in Figure 17(B). Stage (2): the dc field adiabatically changes the electric field to tune the molecular transition through the resonance with relatively strong ac pumping field to produce adiabatic population transfer (see Figure 18(D)) that creates the population inversion between corresponding levels (as shown in Figure 15(e)). Stage (3): the dc field adiabatically changes the electric field to tune the molecular transition till it reaches the resonance with the maser cavity mode (see Figure 18(E,F)). One can see the molecular rotational level structure with, for example,$|\mathrm{m}| = 1$ (see in Figure 19) that can be used for the maser operation. During this stage the microwave amplification occurs depleting all population inversion and then returning to the pumping stage (1).

Using the set of equations for density matrix and the equation for the microwave cavity field, We estimate the gain for some simple molecules such as [25], $\wp \simeq 1\mathrm{D}$ as a typical value, and for frequency $\omega_0 = (2\pi)10$ GHz, and $\mathrm{N} \simeq 2\ 10^{16}\mathrm{cm}^{-3}$ and the gain is of the order of $\mathrm{G} \simeq 2\ 10^{8}\ \mathrm{cm}^{-1}$ correspondingly.

## 3.4 Acknowledgements

We gratefully acknowledge the financial support of the Ministry of Education, Science and Technological Development of the Republic of Serbia (Contract No. 451-03-9/2021-14/200053), and from The Advanced Materials and Manufacturing Processes Institute at the University of North Texas Seed Research Project. Y.R. acknowledges the support from the Fulbright Scholarship, 2021-2022 to Serbia, and he is grateful to the hospitality of the Institute for Multidisciplinary Research, University of Belgrade. We cordially thank Vladimir Sautenkov, Goran Branković, Andrey Matsko, Robert Murawski, and Vyrgil Sanders for fruitful discussions, comments and suggestions.

# CHAPTER 4

# CONCLUSION AND RESULTS

In chapter 2, we consider simple models containing three-level molecules in the $\Lambda$-configuration (see figure 11). We present our study of the excitation of the quantum coherence in a $\Lambda$-type molecular media. We have considered the two- and three-level molecules. The dressed state basis approach is employed, which provides deep physical insights showing interaction of “bright” and “dark” states with radiation. The three-level structure of the model is common for the molecular media, where the split ground states can be viewed for the vibrational level. We have demonstrated the importance of the formulation of dark states between rotational level on Raman and stimulated Raman scattering. We consider the propagation effects for the case when the vibrational coherence is induced. We have considered a gas of three level atoms or molecules in the presence of two coherent optical pulses. The effect of chirp propagation in a dense medium has shown interesting effects. Our model shows interesting behavior in that the population inversion efficiency dies off at some distance and then restores at a later distance and repeats this process with distance. This is different than what has been observed with traditional STIRAP techniques. For our chirp pulse the pulse energy is also transferred from our first to our second pulse. The results of chirp propagation warrant further research and exploration.

The propagation of optical pulse in optically dense medium shows a dependence on effective Rabi frequency. The physics of the formation of dark states is strongly influenced by the presence of the additional excitonic levels. For the case of four-level

scheme we have shown explicitly the dark states that are formed under the action of the laser fields. This is very important for atomic and molecular media and for Raman and coherent Raman spectroscopy. It can also be important for the near field interaction due to a strong electromagnetic field induced by resonant localized plasmons that can result in a strong coupling of excitonic states or formation of hybrid exciton-plasmon modes in quantum confined structures. Silver nanoparticles on molybdenum disulfide (MoS2) is an ideal platform for such interaction (see [70]).

It is remarkable to note here that the CHIRAP can efficiently lead to maximal absorption on one hand, and to creation of population inversion on the other. There are several applications of this swap of populations ranging from nuclear states and gamma radiation [72] to rotational molecular states and microwave radiation [73]. The obtained results are important for applications to manipulation of quantum states for molecular detection in engineering, chemical, and biological applications (see, for example, [32,58,74,75]).

In chapter 3, we develop and demonstrate a new mechanism of manipulation of population in molecular rotational levels in a weakly aligned molecule. Treating molecules as simple rotators, we have described their behavior using the density matrix taking into account the relaxation processes. We consider the interaction of the weakly aligned molecules with a microwave field in a high finesse cavity. Using the mechanism based on an adiabatically changing electric field interacting with the molecules with dipole moments utilizing the transitional dipole moments, we have shown that, on one hand, the population inversion can be reached in the ensemble of the weakly aligned molecules to be used for the maser operation at room temperature. On another hand,

we have found that the enhancement of the absorption can reach the theoretical limit and be used for gas sensing with high sensitivity and selectivity.

It is interesting to note here that the same idea of manipulation of population in molecular rotational levels can be used not only to produce the maser effect, but also to detect signals from molecules for applications in spectroscopy or gas sensing. This technique can work as a sensitive and very selective molecular detector. The resonance depends on the dc electric field applied and the molecular parameters such as rotational constants and the magnitude of the molecular dipole moment. This opens an interesting opportunity of molecular detection at the chosen frequency [7, 8]. Different molecules have their resonances at the chosen frequency but at the different magnitudes of the electric field. Knowing electric field and frequency allows researcher to identify the molecules. This molecular detection is done by way of phase change with the ac sensing field introduced in the model, more precisely by taking the derivative of the phase change. We estimate the sensitivity of the technique for some simple molecules such as [26], using $\wp \simeq 1\mathrm{D}$ as a typical value, and for frequencies $\omega_0 = (2\pi)\, 5$ MHz and 10 GHz, and obtain $\mathrm{N} \simeq 2\ 10^{11}\ \mathrm{cm}^{-3}$ and $\mathrm{N} \simeq 2\ 10^{8}\ \mathrm{cm}^{-3}$ correspondingly. Such sensors can efficiently analyze the multi-gas mixtures and be used for a huge range of applications - stretching from technology, sciences, control of environment, biology and medicine.

REFERENCES

[1] Gordon, J. P.; Zeiger, H. J.; Townes, C. H. (1955). ”The Maser—New Type of Microwave Amplifier, Frequency Standard, and Spectrometer”. Phys. Rev. 99 (4): 1264 (1955) doi:10.1103/PhysRev.99.1264

[2] Mario Bertolotti, The History of the Laser (CRC Press. NewYork, 2004),

[3] Oxborrow, M., Breeze, J. & Alford, N. Room-temperature solid-state maser. Nature 488, 353–356 (2012) doi:10.1038/nature11339

[4] Jonathan D. Breeze, Enrico Salvadori, Juna Sathian, Neil McN. Alford, Christopher W. M. Kay. Continuous- wave room-temperature diamond maser. Nature, 555 (7697): 493 (2018) DOI: 10.1038/nature25970

[5] M. Lemeshko, et al., Manipulation of molecules with electromagnetic fields, MOLECULAR PHYSICS 111, 1648-1682 (2013).

[6] H.J. Loesch, J. Bulthuis, S. Stolte, A. Durand, J.-C. Loison, J. Vigu´e, Molecules Oriented by Brute Force, Europhysics News 27, 12-15 (1996).

[7] Zorica Brankovic, Yuri Rostovtsev, A resonant single frequency molecular detector with high sensitivity and selectivity for gas mixtures, Scientific Reports 10, 1537 (2020).

[8] Yuri Rostovtsev, Zorica Brankovic, A resonant single-frequency molecular detector based on adiabatically changing electric field, Proceedings Volume 11700, Optical and Quantum Sensing and Precision Metrology; 1170018 (2021) https://doi.org/10.1117/12.2586498

[9] E. Arimondo, in Progress in Optics, edited by E. Wolf (Elsevier Science, Amsterdam, 1996), Vol. XXXV, p. 257.

[10] M. O. Scully and M. S. Zubairy, Quantum Optics (Cambridge University Press, Cambridge, England, 1997).

[11] S. E. Harris, Electromagnetically induced transparency, Phys. Today 50, 36 (1997).

[12] M. Fleischhauer, A. Imamoglu, and J. P. Marangos, Electromagnetically induced transparency: Optics in coherent media, Rev. Mod. Phys. 77, 633 (2005).

[13] V.A. Sautenkov, H. Li, Y.V. Rostovtsev, M.O. Scully, Ultradispersive adaptive prism based on a coherently prepared atomic medium, Phys. Rev. A 81, 063824 (2010).

[14] L.V. Hau, S.E. Harris, Z. Dutton, and C.H. Behroozi, Light speed reduction to 17 metres per second in an ultracold atomic gas, Nature 397, 594 (1999);

[15] C. Liu, Z. Dutton, C.H. Behroozi, and L.V. Hau, Observation of coherent optical information storage in an atomic medium using halted light pulses, Nature 409, 490 (2001).

[16] M.M. Kash, V.A. Sautenkov, A.S. Zibrov, L. Hollberg, G.R. Welch, M.D. Lukin, Y. Rostovtsev, E.S. Fry, and M.O. Scully, Ultraslow group velocity and enhanced nonlinear optical effects in a coherently driven hot atomic gas, Phys. Rev. Lett. 82, 5229 (1999). D. Budker, D.F. Kimball, S.M. Rochester, and V.V. Yashchuk, Phys. Rev. Lett. 83, 1767 (1999).

[17] L.J. Wang, A. Kuzmich, and A. Dogariu, Gain-assisted superluminal light propagation, Nature (London) 406, 277 (2000); A. Dogariu, A. Kusmich, and L.J. Wang, Transparent anomalous dispersion and superluminal light-pulse propagation at a negative group velocity. Phys. Rev. A 63, 053806 (2001).

[18] G. S. Agarwal, T. N. Dey, and S. Menon, Knob for changing light propagation from subluminal to superluminal, Phys. Rev. A 64, 053809 (2001).

[19] E.E. Mikhailov, V.A. Sautenkov, Y.V. Rostovtsev, and G.R.Welch, Bu er-gas-induced absorption resonances in Rb vapor, J. Opt. Soc. Am. B 21, 425 (2004);

[20] Q. Sun, Y.V. Rostovtsev, J.P. Dowling, M.O. Scully, and M. S. Zubairy, Optically controlled delays for broadband pulses, Phys. Rev. A 72, 031802 (2005).

[21] Dmitry Pestov, Robert K Murawski, Gombojav O Ariunbold, Xi Wang, Miaochan Zhi, Alexei V Sokolov, Vladimir A Sautenkov, Yuri V Rostovtsev, Arthur Dogariu, Yu Huang, Marlan O Scully, Optimizing the laser-pulse configuration for coherent Raman spectroscopy, Science 316, 265-268 (2007).

[22] A.R. Edmonds, Angular Momentum in Quantum Mechanics, Series: Investigations in Physics (PRINCETON UNIVERSITY PRESS, Princeton, 1996),

[23] H.-P. Breuer, F. Petruccione, The theory of open quantum systems, Oxford University Press Inc., New York 2006.

[24] E.G. Warburg, Magnetische Untersuchungen über einige Wirkungen der Coerzitivkraft, Annalen der Physik (Leipzig) 13, p. 141-164, (1881).

[25] Pierre Weiss, Auguste Piccard, "Le phnenomene magnetocalorique". J. Phys. (Paris). 5th Ser. (7), 103{109 (1917).

[26] Anders Smith, Who discovered the magnetocaloric effect? The European Physical Journal 38, (4): 507-517, (2013).

[27] R.W. Boyd, Nonlinear optics (Boston, Academic Press, 1992).

[28] Y.R. Shen, The principles of nonlinear optics (New York, J. Wiley, 1984).

[29] Infrared and Raman Spectroscopy, Ed. B. Schrader (VCH, Tokyo, 1995).

[30] A. K. Patnaik, I. V. Adamovich, J. R. Gord, and S. Roy, "Recent Advances in ultrafast-laser-based spectroscopy and imaging for reacting plasmas and flames," Plasma Sources Science and Tech 26, 103001 (2017).

[31] T. Lang, M. Motzkus, Single-shot femtosecond coherent anti-Stokes Raman-scattering thermometry. J Opt Soc Am B 19, 340{4 (2002).

[32] A. K. Patnaik, S. Roy, and J. R. Gord, “Ultrafast saturation of resonant optical processes," Phys. Rev. A 90, 063813 (2014).

[33] M.O. Scully, G.W. Kattawar, B.P. Lucht, Opatrny T, Pilloff H, Rebane A, A. V. Sokolov, M.S. Zubairy, “FAST CARS: Engineering a laser spectroscopic technique for rapid identification of bacterial spores," PNAS 99, 10994 (2002).

[34] D. Pestov, M.C. Zhi, Z.-E. Sariyanni, N.K. Kalugin, A.A. Kolomenskii, R. Murawski, G.G. Paulus, V.A. Sautenkov, H. Schuessler, A.V. Sokolov, G.R. Welch, Y.V. Rostovtsev, T. Siebert, D.A. Akimov, S. Graefe, W. Kiefer, M.O. Scully, “Visible and UV coherent Raman spectroscopy of dipicolinic acid," PNAS 102, 14976-14981 (2005).

[35] Fa-Ke Lu, Minbiao Ji; Dan Fu, Xiaohui Ni, Christian W. Freudiger, Gary Holtom, X. Sunney Xie, “Multicolor stimulated Raman scattering microscopy," Mol. Phys. 110, 1927-1932 (2012).

[36] Dan Fu, Gary Holtom, Christian W. Freudiger, X. Zhang, X. S. Xie, “Hyperspectral Imaging with Stimulated Raman Scattering by Chirped Femtosecond Lasers," J. Phys. Chem. B 117, 4634 (2013).

[37] S.Roy, J.R. Gord, A.K. Patnaik, “Recent advances in coherent anti-Stokes Raman scattering spectroscopy: Fundamental developments and applications in reacting flows," Prog. Energy Combust. Sci. 36. 280 (2010).

[38] "Short Pulse Laser Interactions with Matter," P. Gibbon (Imperial College Press, 2005).

[39] S. E. Harris, “Electromagnetically induced transparency with matched pulses," Phys. Rev. Lett. 70, 552 (1993).

[40] O. Kocharovskaya, and Ya.I. Khanin, “Population trapping and coherent bleaching of a three-level medium by a periodic train of ultrashort pulses," Sov. Phys. JETP 63, 945 (1986).

[41] V.A. Sautenkov, Y.V. Rostovtsev, C. Y. Ye, G.R. Welch, O. Kocharovskaya, and M.O. Scully, “Electromagnetically induced transparency in rubidium vapor prepared by a comb of short optical pulses," Phys. Rev. A 71, 063804 (2005).

[42] A.K. Patnaik, P. Hsu, G.S. Agarwal, G. Welch, M.O. Scully, Measurement of ground state decoherence via interruption of coherent population trapping, Physical Review A, 75 (2007) 023807.

[43] A.K. Patnaik, G.S. Agarwal, C.H.R. Ooi, M.O. Scully, Quantum correlation between a pair of Raman photon from single atom under arbitrary excitation condition, Physical Review A, 72 (2005) 043811.

[44] E. Paspalakis, N. J. Kylstra, and P. L. Knight, "Propagation and nonlinear generation dynamics in a coherently prepared four-level system," Phys. Rev. A 65, 053808 (2002);

[45] P.S. Hsu, G.R. Welch, J.R. Gord, A.K. Patnaik, "Propagation dynamics of controlled cross-talk via interplay between $\chi^1$ and $\chi^2$ processes," Phys Rev A, 83053819 (2011).

[46] F. Abeles, Optical properties of solids (Amsterdam, North-Holland Publishing Company, 1972).

[47] Q. Sun, Y.V. Rostovtsev, J.P. Dowling, M.O. Scully, and M. S. Zubairy, “Optically controlled delays for broadband pulses," Phys. Rev. A 72, 031802 (2005).

[48] A. B. Matsko, Y. V. Rostovtsev, M. Fleischhauer, and M. O. Scully, \Anomalous Stimulated Brillouin Scattering via Ultraslow Light," Phys. Rev. Lett. 86, 2006 (2001).

[49] Y.V. Rostovtsev, Z.-E. Sariyanni, and M.O. Scully, “Electromagnetically Induced Coherent Backscattering," Phys. Rev. Lett. 97, 113001 (2006).

[50] L. Allen and J. H. Eberly, Optical Resonance and Two Level Atoms (Dover, 1987).

[51] D. Sun, Z.-E. Sariyanni, S. Das, and Y.V. Rostovtsev, “Propagation of 0 pi pulses in a gas of three-level atoms," Phys. Rev. A 83, 063815 (2011).

[52] Z.-E. Sariyanni, D. Sun, and Y.V. Rostovtsev, “Stimulated Raman spectroscopy with 0 pi pulses," Opt. Lett. 39, 766-768 (2014).

[53] N.V. Vitanov, A.A. Rangelov, B.W. Shore, K. Bergmann, “Stimulated Raman adiabatic passage in physics, chemistry, and beyond," Re, Mod. Phys. 89, 015006 (2017).

[54] N.V. Vitanov, M. Fleischhauer, B.W. Shore, K. Bergmann, The advances in Atomic, Molecular, and Optical Physics 46, 55 (2001), edited by B. Bederson and H. Walther.

[55] R. Netz, A. Nazarkin, and R. Sauerbrey, “Observation of Selectivity of Coherent Population Transfer Induced by Optical Interference," Phys. Rev. Lett. 90, 063001 (2003).

[56] T. A. Collins, S. A. Malinovskaya, “Manipulation of ultracold Rb atoms using a single linearly chirped laser pulse," Opt. Lett. 37, 2298 (2012).

[57] S. A. Malinovskaya, “Prevention of decoherence by two femtosecond chirped pulse trains", Optics Lett. 33, 22452247 (2008).

[58] Regina de Vivie-Riedle and Ulrike Troppmann, Femtosecond Lasers for Quantum Information Technology, Chem. Rev. 107, 11, 5082{5100 (2007).

[59] G.P. Djotyan et al.: Three-level Lambda atom in the field of frequency-chirped bichromatic laser pulses, Writing and storage of optical phase information, PRA, 64, 013408 (2001)

[60] G.P. Djotyan, et al., Coherent control of atomic quantum states by single frequency-chirped laser pulses" PRA, 70, 063406 (2004)

[61] G. Demeter et al. Propagation of frequency-chirped laser pulses in a medium of atoms with a Lambda-level scheme. PRA, 76, 023827 (2007).

[62] G.P. Djotyan, et al. Creation of a coherent superposition of quantum states by a single frequency-chirped short laser pulse. JOSA B, 26, n.2, p. 166-174 (2008).

[63] N Sandor et al.; Creation of coherent superposition states in inhomogeneously broadened media with relaxation JOSA B-OPTICAL PHYSICS, 28, Pages: 2785-2796 (2011)

[64] N. Sandor, et al., Coherence creation in an optically thick medium by matched propagation of a chirped-laser-pulse pair, PRA 89, 033823 (2014).

[65] Y. Rostovtsev, I. Protsenko, H. Lee, and A. Javan, “From laser-induced line narrowing to electromagnetically induced transparency in a Doppler-broadened system," J. Mod. Opt. 49, 2501 (2002);

[66] H. Lee, Y. Rostovtsev, C.J. Bednar, and A. Javan, “From laser-induced line narrowing to electromagnetically induced transparency: closed system analysis," Appl. Phys. B 76, 33 (2003);

[67] A. K. Patnaik, G. S. Agarwal, "Coherent control of magneto-optical rotation in inhomogeneously broadened medium" Optics Communications 199, 127-142 (2001).

[68] P. Singh, A.K. Patnaik, S. Roy, J.R. Gord, Y.V. Rostovtsev, "Influence of coherent population trapping on Raman scattering," Physical Review A 100 (2), 023808 (2019).

[69] A. K. Patnaik, S. Roy, and J. R. Gord, “Saturation of vibrational coherent anti-Stokes Raman scattering mediated by saturation of the rotational Raman transition," Phys. Rev. A 87, 043801 (2013).

[70] Y. Poudel, G. N. Lim, M. Moazzezi, Z. Hennighausen, Y. Rostovtsev, F. DSouza, S. Kar, A. Neogi, "Active control of coherent dynamics in hybrid plasmonic MoS2 monolayers with dressed phonons," arXiv:1810.02056 [condmat.mes-hall] (2018).

[71] Z. Brankovic, Y. Rostovtsev, "A resonant single frequency molecular detector with high sensitivity and selectivity for gas mixtures," Sci. Rep. 10, 1537 (2020).

[72] C. D. Roy, A. K. Patnaik, and Y. Rostovtsev, "Controlling polarization of the gamma-rays via chirped RF pulses," Phys. Rev. (in preparation, 2022).

[73] C. D. Roy, Z. Brankovic, and Y. Rostovtsev, Weakly Aligned Molecules: From Molecular Detectors to Room Temperature Tunable Masers, Journal of Physics: Conference Series 2249 (1), 012001 (2022).

[74] Anil K. Patnaik, Sukesh Roy, and James R. Gord, “Ultrafast saturation of electronic-resonance-enhanced coherent anti-Stokes Raman scattering and comparison for pulse durations in the nanosecond to femtosecond regime," Phys. Rev. A 93, 023812 (2016)

[75] A. K. Patnaik, S. Roy, and J. R. Gord, "Lineshape dependence of ultrafast saturation of absorption and fluorescence," Physica Scripta T165 014031 (2015).

[76] S. Alam, Lasers without Inversion and Electromagnetically Induced Transparency (SPIE Optical Engineering Press, Bellingham, Washington, USA, 1999).